INVESTIGATION OF THE FUNCTIONS OF NEW GENES INVOLVED IN REPAIR OF DNA DOUBLE-STRAND BREAKS IN *SACCHAROMYCES CEREVISIAE*

by

Brian A. Sanderson, B.S.

A thesis submitted to the Graduate Council of
Texas State University in partial fulfillment
of the requirements for the Degree of
Master of Science
with a Major in Biochemistry
December 2013

Committee Members:

L. Kevin Lewis, Chair

Corina Maeder

Rachell Booth

FAIR USE AND AUTHOR'S PERMISSION STATEMENT

Fair Use

Duplication Permission

ACKNOWLEDGEMENTS

I would like to begin by thanking everyone that has supported me and helped me achieve my goals thus far. Dr. Kevin Lewis, for giving me the support and guidance to get where I am today. Thank you for your patience and for giving me the opportunity to work on so many projects. To Dr. Gary Beall for opening his door and giving me my first research project. I would also like to thank my committee members, Dr. Corina Maeder and Dr. Rachell Booth, for their advice and comments throughout this process. Whitney Wood, Jennifer DeMars Tripp, Eric Malczewskyj, and to everyone else that has been part of the Lewis lab, it has been fun and I wish you all the best of luck in the future. Thank you to all the friends that I have met along the way. To my brothers for motivating me to be the first family member to earn a master's degree. Finally, I would like to thank my mother and father for all the support they have given me during my life endeavors.

TABLE OF CONTENTS

Page

ACKNOWLEDGEMENTS iv

LIST OF TABLES vi

LIST OF FIGURES vii

CHAPTER

I. INTRODUCTION 1

II. MATERIALS AND METHODS 10

III. RESULTS AND DISCUSSION 18

IV. SUMMARY AND CONCLUSIONS 43

REFERENCES 46

LIST OF TABLES

Table **Page**

1. Oligonucleotides used for PCR reactions 14

2. Survival of the 48 new mutants after exposure to EcoRI, MMS, bleomycin, and gamma radiation 19

3. Results from the plasmid:chromosome recombination assay of *rad57* and the 48 new mutants 21

4. Results from the qualitative intrachromosomal recombination assay of RAD52 and non-RAD52 group mutants 26

5. Results from the quantitative intrachromosomal recombination assay of RAD52 and non-RAD52 group mutants 28

6. Rates of intrachromosomal recombination for library *MATα* DUBm mutants 30

7. EcoRI, MMS, and bleomycin sensitivity results for DUBm mutants created using PCR-mediated gene disruption 36

8. Median frequencies of 5-FOA^r, 5-FOA^r Leu$^-$, 5-FOA^r Leu$^+$ Ade$^-$, and 5-FOA^r Leu$^+$ Ade$^+$ cells 42

LIST OF FIGURES

Figure **Page**

1. Illustration of EcoRI cleavage of double-stranded DNA 3

2. Schematic of non-homologous end-joining repair pathway in the model eukaryote *Saccharomyces cerevisiae* (budding yeast) (3) 4

3. Illustration of the homologous recombination repair pathway in the model eukaryote *Saccharomyces cerevisiae* (budding yeast) 6

4. Expression of EcoRI inside yeast cells using a galactose-regulated promoter 8

5. Plasmid recombination assay for repair of a site-specific DSB on a plasmid 20

6. Schematic representation of direct repeat intrachromosomal recombination on chromosome XV 22

7. Illustration of replica-plating assay (22) 23

8. Testing RAD52 group mutants for intrachromosomal recombination efficiency on YPDA (left) and 5-FOA (right) plates 24

9. Replica plates of recombinant cells on YPDA (left square) and 5-FOA (right square) plates 25

10. Survival of haploid library *sgf11*, *sgf73*, and *sus1* mutants after induction of EcoRI expression 30

11. Example PCR amplification of the G418^r gene (~1.2 kb) using *ubp8* primers gubp8a and gubp8b 31

12. Agarose gel electrophoresis of PCR fragments from G418^r genomic DNA 32

13. PCR confirmation of DUBm gene knockouts 33

14. Survival of DUBm mutants after EcoRI expression *in vivo* 34

15. Pronging of DUBm mutants to measure sensitivity to 2 and 4 μg/ml bleomycin 35

16. Pronging assays showing that MMS has no effect on DUBm mutants that were constructed in this study 36

17. Schematic representation of LOH assays 38

18. PCR amplification of *URA3* from plasmid DNA and confirmation of *URA3* insertion into genomic DNA 39

19. Schematic representation of loss of heterozygosity events on chromosome III 41

CHAPTER I

Introduction

Deoxyribonucleic acid (DNA) is the hereditary material that contains the genetic information that living organisms use for development and function. This information is encoded into sequences of four nitrogenous bases: adenine (A), guanine (G), cytosine (C), and thymine (T). Each base is attached to a sugar-phosphate backbone, which makes up one nucleotide. A DNA strand is formed by joining nucleotides together. Each strand forms hydrogen bonds with an anti-parallel complementary strand (A to T and C to G). Double-stranded DNA further obtains a helical structure through base stacking. Double-helical DNA may exist as circular or long linear polymers within cells.

DNA located in eukaryotic cells is constantly exposed to DNA damaging agents that result in the formation of multiple types of lesions. DNA lesions can occur exogenously by exposure to ionizing radiation and chemicals such as bleomycin and methyl methanesulfonate (MMS) or endogenously via free radicals and with endonucleases such as EcoRI (1). The types of DNA lesions that occur include damaged bases, sugar alterations, and single-strand or double-strand breaks (DSBs) (2).

Ionizing radiation can damage DNA by direct and indirect actions (3). Direct actions occur from direct absorption of radiation energy by DNA, causing ionization of bases or sugars. Indirect damage occurs when DNA interacts with reactive oxygen species (hydroxyl radicals, superoxide anion radicals, etc.) that form in water by radiation. Radiation can cause DNA strand breaks and other lesions such as base change or loss that occur on either a single strand or on both strands.

Bleomycin is a naturally occurring glycopeptide isolated from *Streptomyces verticillis* that is used as an antitumor drug that causes DNA double-strand breaks (DSBs) and other lesions (4). DNA cleavage occurs after the chemical chelates metal ions, creating a pseudo-enzyme that reacts with oxygen to produce hydroxyl free radicals and superoxides that attack DNA (5). Bleomycin contains a metal binding site for iron, a glycol-peptide that binds to a sugar and sits in the minor groove, and an end that intercalates into DNA. MMS is another DNA damaging agent that methylates DNA at N7-deoxyguanine and N3-deoxyadenine (6). The resulting 3-methyladenine stalls replication forks, resulting in single-strand breaks (SSBs). Two SSBs that occur in close proximity of each other on complementary DNA strands can resemble a DSB (7).

Restriction endonucleases catalyze the hydrolysis of phosphodiester bonds within the interior of DNA, creating a DSB. Many of the enzymes recognize specific palindromic sequences that are typically 4, 6, or 8 bp in length (8). Currently, restriction endonucleases are categorized into 4 main types (Types I, II, III, and IV) based on structure, recognition sequence, and position of cleavage within the recognition sequence (8, 9). Type II enzymes are the most extensively studied and the largest class of restriction enzymes. Type II restriction enzymes can either produce single-stranded DNA overhangs (3' or 5') or blunt DNA ends. Enzymes that produce 5' single-strand overhangs approach the recognition sequence from the major groove whereas endonucleases that produce 3' or blunt ends approach DNA from the minor groove (8, 10).

EcoRI is a type II restriction enzyme that has the recognition sequence G^AATTC (Figure 1). It has been expressed from a galactose-regulated promoter in yeast

cells to study cellular responses and repair of DSBs *in vivo* (11–13). Unlike radiation, MMS, and bleomycin, EcoRI is believed to only produce DSBs. DSBs are the most detrimental type of DNA lesion; causing mutations, loss of cell function, and cell death if left unrepaired or repaired incorrectly (2, 14).

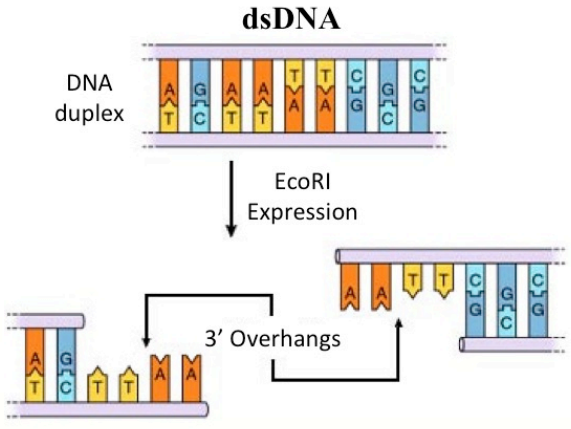

Figure 1. Illustration of EcoRI cleavage of double-stranded DNA.

In response to DSBs, eukaryotic cells utilize two highly conserved independent repair mechanisms: non-homologous DNA end joining (NHEJ) and homologous recombination (HR) (14, 15). NHEJ, schematically shown in Figure 2, is an error-prone repair pathway that is the primary pathway in humans and the secondary pathway in yeast. Repair by NHEJ does not use a homologous chromosome as a template, but does require three protein complexes: the Yku70/Yku80, Mrx, and DNA Ligase IV complexes. The Yku70/Yku80 complex binds to DNA ends and protects them from nucleases. Mrx tethers the broken DNA ends together using Mre11, Rad50, and Xrs2 proteins. Finally, DNA Ligase IV, made of Dnl4, Lif1, and possibly Nej1, covalently links broken DNA strands together.

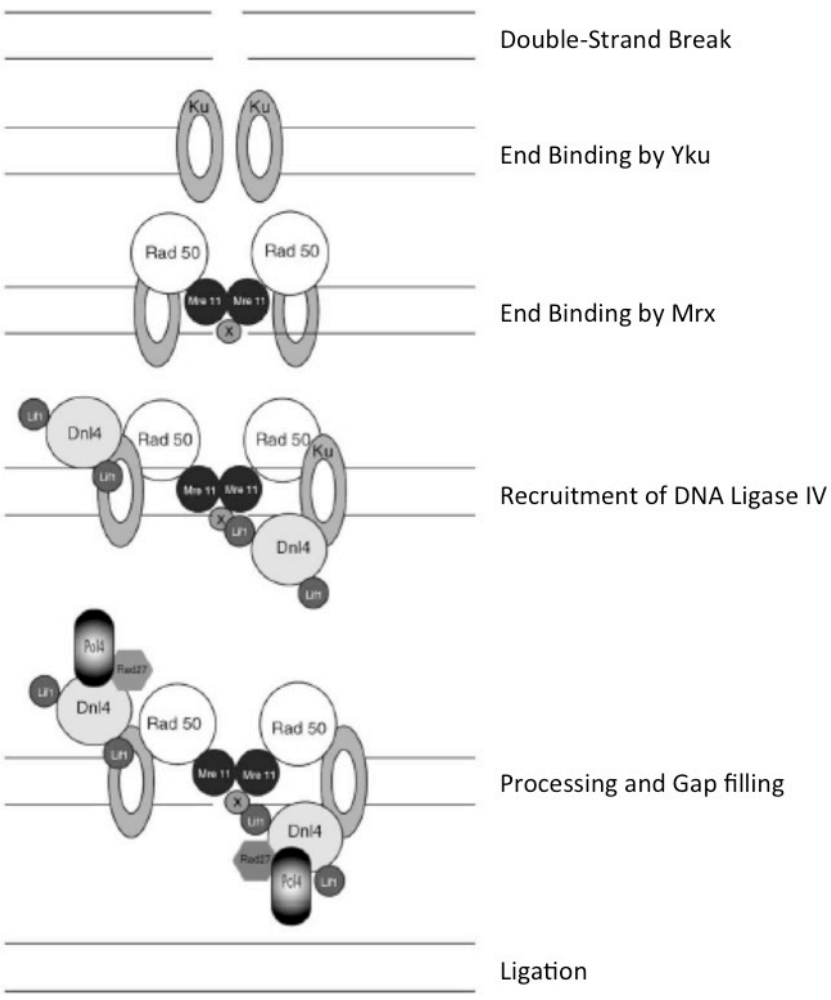

Figure 2. Schematic of non-homologous end-joining repair pathway in the model eukaryote *Saccharomyces cerevisiae* (budding yeast) (3).

Homologous recombination involves a multi-step process that requires substantial energy and uses multiple proteins with homologous chromosomes in the same cell to repair damaged DNA (Figure 3). The use of homologous chromosomes as a template for repair makes this process virtually error free (16, 17). This pathway requires several proteins that are not found in NHEJ, which include Rad51, Rad52, Rad54, Rad55, Rad57, and Rad59 (16). HR is initiated with the resection of DSB ends by Mrx and other proteins

such as Exo1, Sae2, Sgs1, and Dna2 to create long 3' single-strand overhangs on both strands of DNA at the break site. The single-stranded DNA (ssDNA) binding complex Rpa and other proteins such as Rad51, Rad52, Rad54, Rad55, Rad57, and Rad59 are recruited for homology search, strand invasion and exchange with homologous chromosomes. The final steps include DNA replication, branch migration, nucleosome assembly, and resolution, producing a repaired chromosome. The pathway also includes several additional proteins that are involved in DNA damage checkpoint responses, nucleosome remodeling, sister chromatid cohesion, and other processes involving nucleases, resolvase-like enzymes, and chromatin reassembly proteins (16, 17).

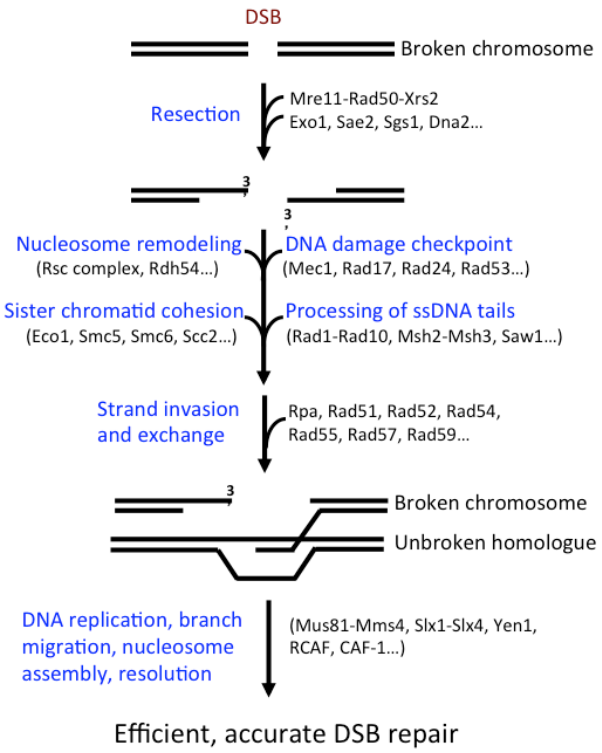

Figure 3. Illustration of the homologous recombination repair pathway in the model eukaryote *Saccharomyces cerevisiae* (budding yeast).

Cells contain checkpoint mechanisms that monitor DNA integrity. When damaged DNA passes through the cell cycle checkpoints, a large number of checkpoint genes arrest the cell cycle in G_2 phase and provide time for repair of the damaged DNA before completing the cell cycle (18, 19). Exposure to DNA damaging agents such as MMS and ionizing radiation results in prolonged cell cycle arrest in yeast cells that are recombination-deficient such as *rad51* and *rad52* cells.

Unicellular lower eukaryotes, such as the yeast *Saccharomyces cerevisiae,* are often used as model organisms to analyze genetic factors that contribute to cell function and survival. Yeast cells are ideal because they are grown rapidly in the laboratory and contain genes homologous to those in humans, which are multicellular higher eukaryotes.

Unlike multicellular organisms, yeast cells can grow as either haploid or diploid, which allows for rapid and precise analysis of gene mutations.

Yeast deletion strain libraries provide a way to screen multiple mutants for a particular phenotype. These libraries contain about five thousand yeast mutants, each with one non-essential gene inactivated (20, 21). The coding sequence of each non-essential gene was replaced with a gene encoding resistance to the antibiotic G418 (20). The mutants are stored indefinitely at -80 °C in nutrient-rich broth and glycerol in 96-well microtiter dishes.

Two previous studies by Bennett *et al.* and Game *et al.* screened diploid yeast deletion libraries for gamma radiation-sensitivity (20, 21). Bennett *et al*. initially identified 200 gamma sensitive mutants. Eight of the genes were part of the RAD52 group (*RAD50, RAD51, RAD52, RAD54, RAD55, RAD57, MRE11, and XRS2*) and were known to affect DSB repair. Game *et al.* then identified 33 genes required for normal resistance to radiation, 11 of which were not previously identified by Bennett *et al.* These two screens identified a total of 211 gamma-sensitive mutants. The 211 mutants were then screened in the Lewis lab for sensitivity to DSBs produced by *in vivo* expression of EcoRI endonuclease using a *GAL1* promoter, whose 6 bp target sequence is present in more than 2000 copies in the yeast genome (Figure 4). Previous graduate students Jennifer Summers, Sunaina Sethi, and Jennifer DeMars performed EcoRI sensitivity assays using haploid library mutants of both mating types (yeast cells can exist as *MAT*α or *MATa* cells) (22-24). Eighty-one of the 211 mutants were identified as EcoRI-sensitive. Only a few of these mutants were previously linked to DNA repair, while the remaining genes are new. Most of the 81 EcoRI^s mutants were also killed by exposure to

the DNA damaging chemicals bleomycin and MMS. Forty-eight of the identified genes are involved in nuclear processes where DNA repair occurs, including several associated with chromatin structure, nucleosome remodeling, sister chromatid cohesion, and transcription.

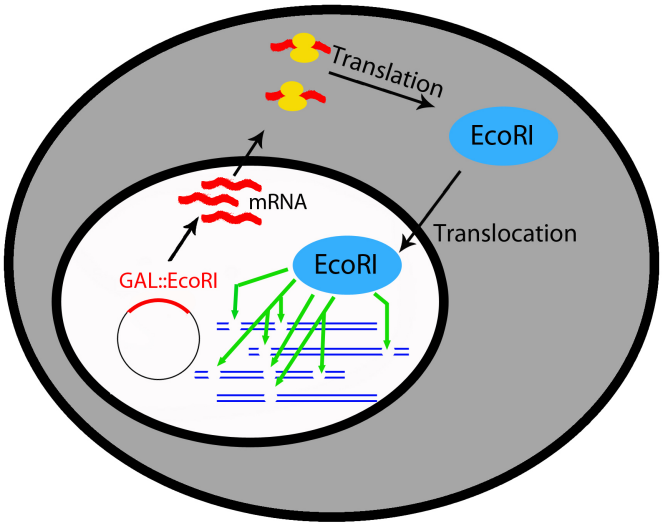

Figure 4. Expression of EcoRI inside yeast cells using a galactose-regulated promoter.

The yeast Ubp8 protein removes ubiquitin groups from histone proteins and some protein kinases, causing alterations of chromatin structure in promoter regions and facilitating transcription of several genes. It contains the active site for the deubiquitination module (DUBm) within the SAGA (Spt-Ada-Gcn5-Acetyltransferase) histone acetylation complex. Ubp8 is a protease that cleaves monoubiquitin from lysine-123 of histone H2B during transcription elongation (25, 26). Full enzymatic activity of Ubp8 requires three additional proteins, Sgf73, Sgf11, and Sus1 (25, 27). Ubp8 and Sgf11 are both thought to be involved in the cleavage of monoubiquitin, while Sgf73 is responsible for binding the DUBm complex to SAGA and is also involved in molecular export of mRNAs in conjunction with Sus1 (28, 29).

In the current project, 48 new non-RAD52 group genes required for resistance to EcoRI have been characterized for their role in DNA DSB repair. Assays were developed and used to investigate interchromosomal and intrachromosomal homologous recombination. Several *in vivo* systems were designed and tested to monitor chromosome stability and loss of heterozygosity (LOH). The best LOH system was used to investigate the roles of Ubp8, Sgf73, Sgf11, and Sus1 in chromosome stability.

CHAPTER II

Materials and Methods

I. Materials

General reagents

Methylmethane sulfonate (MMS), dimethyl sulfoxide (DMSO), ampicillin, RNase A, and lithium acetate were purchased from Sigma-Aldrich Chemical Co. (St. Louis, MO). Ethylenediaminetetraacetic acid (EDTA), agarose, and bleomycin were purchased from EMD Chemicals, Inc. (Darmstadt, Germany). A standard 2-log DNA ladder was purchased from New England Biolabs (Beverly, MA). Ethidium bromide (EtBr) was obtained from Shelton Scientific, Inc. (Shelton, CT). Polyethylene glycol (PEG) 4000, sodium dodecyl sulfate (SDS), sodium chloride, and boric acid were purchased from Mallinckrodt (Paris, KY). Sonicated salmon sperm carrier DNA was purchased from Stratagene (La Jolla, CA). Tris base was obtained from VWR International (West Chester, PA). Dithiothreitol (DTT) and 5-fluoroorotic acid were purchased from Gold Biochemistry (St. Louis, MO).

Yeast strains and plasmids

Initial studies utilized haploid *MATa* and *MATα* yeast deletion strain libraries obtained from Open Biosystems (Huntsville, AL). The library mutants were derived primarily from BY4741 (*MATa ura3Δ0 leu2Δ0 his3Δ1 met17Δ0*) and BY4742 (*MATα ura3Δ0 leu2Δ0 his3Δ1 lys2Δ0*) (8). YKU23 (*MAT*α *lys2*Δ*202 leu2*Δ*1 ura3-52 his3*Δ*200 ade2*Δ*::hisG)* and YKU34 (*MAT*a *lys2*Δ*202 leu2Δ1 ura3-52 trp1*Δ*63 III-205::URA3*

*ade2*Δ*::hisG III-314::ADE2 LEU2)* were provided by Dr. Hisaji Maki (Nara Institute of Science and Technology) for LOH assays. New mutants were constructed by PCR-mediated gene disruption-deletion using pFA6MX4 and insertion of a gene encoding G418 resistance (30). Plasmids in the study included pRS315 (*CEN/ARS LEU2*), pRS316 (*CEN/ARS URA3*), pGALEcoRI (YCpGAL::RIb) (*CEN/ARS URA3 GAL1p::EcoRI*), pRS306 (*URA3*), and pLKL37Y (*HIS3 URA3*).

Yeast growth media

Difco bacto peptone, bacto yeast extract, bacto tryptone, bacto agar, yeast nitrogen base and LB broth mix were obtained from Becton Dickinson Microbiological Systems (Sparks, MD). D-(+)-galactose, D-(+)-glucose, raffinose, and amino acids were purchased from Sigma-Aldrich Chemical Co. (St. Louis, MO). For non-selective growth, yeast cells were grown on YPDA plates (1% bacto yeast extract, 2% bacto peptone, 2% glucose, 2% bacto agar, 0.001% adenine). YPDA liquid media was prepared as plate media without agar. Mitochondrial function was determined by growing yeast cells on YPG (1% bacto yeast extract, 2% bacto peptone, 2% bacto agar, 3% v/v glycerol). Plasmid selection was completed by growing yeast cells on synthetic media with drop-out mix (0.17% yeast nitrogen base without amino acids, 2% glucose, 2% bacto agar, and all essential amino acids and bases minus those used for selection). Glucose complete (2%), raffinose (2%), and galactose (3%) plates were made using synthetic media. MMS plates were made using YPDA supplemented with aliquots of a stock solution of 11.2 M MMS. Plates with bleomycin were prepared using synthetic media supplemented with aliquots from a stock solution of 0.5 mg/ml bleomycin in ddH_2O. Plates with 5-FOA were prepared as synthetic media with a final concentration of 1 mg/ml 5-FOA. *E. coli* cells

were grown in LB + ampicillin (Amp) broth (1% bacto tryptone, 0.5% yeast extract, 0.5% NaCl, 100 μg/ml ampicillin) or on LB + Amp plates (as broth, with 1.5% agar).

II. Methods

Plasmid DNA purification

Purification of plasmid DNA was achieved using a Qiaprep Spin Miniprep kit (Qiagen; Maryland, VA).

Gel electrophoresis

Gel electrophoresis was performed using 0.8%-1.2% agarose gels in 1X TAE (40 mM Tris base, 20 mM acetic acid, 1 mM EDTA) running buffer in a Life Technologies Horizon 11-14 gel rig at a voltage of ~140 V and stained with 0.5 μg/ml EtBr for 20 min. A Kodak IS440 CF Imager and Carestream imaging software were used to capture gel images.

Yeast transformations

Routine transformations of plasmid DNA into yeast cells were performed using a modified version of the rapid lithium acetate/DMSO-based transformation protocol of Soni *et al.* (31). Some transformations used the higher efficiency protocols of Gietz *et al.* (32) or Tripp *et al*. (33).

Targeted gene disruption

DNAs used for gene disruptions were PCR-amplified in 50 μL reactions containing 1X ThermoPol Reaction Buffer, 0.25 mM dNTPs, 5 U Taq DNA Polymerase (New England Biolabs Inc.), 1 μM of each primer (Life Technologies), and 2 μl of

plasmid or chromosomal DNA template. PCR was initiated with a 2 min 94 °C denaturation, followed by 32 cycles of 95 °C for 30 s, 54 °C for 40 s, 72 °C for 1 min, and terminated with a 7 min 72 °C extension. Annealing temperatures were sometimes varied to improve yields. The PCR products were then analyzed by gel electrophoresis and transformed into yeast cells using the modified Soni *et al.* protocol (31). Correct integration of DNA was verified by first selecting on synthetic plates and then by extracting genomic DNA from colonies using either the protocol of Lõoke *et al*. (34) or Lee *et al.* (35). DNA was PCR-amplified using the same conditions previously described with the exception of a 56 °C annealing temperature. Ex Taq Polymerase (TaKaRa Bio Co.- Mountain View, CA) was used for deletion of *RAD52* because Taq Polymerase did not work well with *RAD52* primers. Oligonucleotides used for PCR reactions are shown in Table 1.

The modified Lõoke *et al.* protocol used here was performed as follows:

1. Pick one yeast colony from the plate or spin down 100-200 μl of liquid yeast culture (OD_{600}=0.4). Suspend cells in 100 μl of 200 mM LiOAc, 1% SDS solution.
2. Incubate for 5 min at 70 °C.
3. Add 300 μl of 96-100% ethanol, vortex.
4. Spin down DNA and cell debris at 15,000 g for 3 min.
5. Wash pellet with 200 μl 70% ethanol.
6. Dissolve pellet in 50 ml of TE and spin down cell debris for 15 s at 15,000 g.
7. Remove 2 μl for PCR reactions.

Table 1. Oligonucleotides used for PCR reactions.

Primer	Sequence
pTYR1A	GAATACCGTAGCACTTGAAGGAAAGAGGACAGCATATCCACTTGATAAACATGGCAGAGCAGATTGTACTGAGAGTGCACC
pTYR1B	CATTATGTATTTCTTTTTTCAGCGGCCGAACGGTCACTAGAATGACTCAGAATGGCGCATCTGTGCGGTATTTCACACCGC
5'Tyr1	CCTCTAATAAGCGTTATACCAGTGTAGTA
3'Tyr1	ACGATAATCGCGGTAGTGAGCATTACACA
pGAL2A	CATAATGGCAGTTGAGGAGAACAATATGCCTGTTGTTTCACAGCAACCCCAAGCCAGAGCAGATTGTACTGAGAGTGCACC
pGAL2B	AGAGATGATGGAGCGTCTCACTTCAAACGCATTATTCTAGCATGGCCTTGTACCCGCATCTGTGCGGTATTTCACACCGC
5'Gal2	ATACAACATTCTGGAGAGCTATTGTTCAA
3'Gal2	ATAATCGTAAGGATATCATTGATAAGGGA
pBOI1A	GTTTACGAATTAATACAATCAAATTAGACACTGATACTATCAAGAAGTACATCGCAG CAGAGCAGATTGTACTGAGAGTGCACC
pBOI1B	CAATAATAATAATATATATATCCAGTAATTTGAAAGAAGAGGACATCATGTCTGCGGTTCCGCATCTGTGCGGTATTTCACACCGC
5'Boi1	CTGCAATCATTAGTTACTTCTTGACCA
3'Boi1	TAAACGCAGGTTGGCCAAAACATAACA
pEMC6A	GACATGACAACAGTATTCTCAGTCAAATGATTTCAAATACACAATGTTAAATTCTCCAGAGCAGATTGTACTGAGAGTGCACC
pEMC6B	CCTACTTTTTGTACCTCATCTCTATTTTTCTGCAAAAATCTTTGCGCTCTTACGCTCCGCATCTGTGCGGTATTTCACACCGC
5'Emc6	TTGGTTCCTGATTCTGTACAACTTGAT
3'Emc6	GTGAGGGTAAGAAATTGATCGTCATTGC
gUBP8a	GTATTGGGACGACGTGTGCACAAAGACCATGGTTCCTAGCATGGAAAGAAGAGATGATGTGACTGTCGCCCGTACATT
gUBP8b	CAATAGACCTTTCCAAGGAGCCCTCAAACACAGTATGCACTATGCATTCACACTGCGACAAGTTCTTGAAAACAAGAATC
5'Ubp8	AACTACAGCTTCGGTCCTCGTCGTCCT
3'Ubp8	TACAGTATATGCACAATCGCAACTCAT
gSGF73a	CCCAACTGAAAAGCATTTAATTGATTTCAACAAACAGTGTGGTGTAGAGTTGCCATGTGACTGTCGCCCGTACATT
gSGF73b	CCATTTAGAACCTGTGTTGTTTCCTCTTCAGGAGTTAGGTTAACGTGTCCTATCACAAGTTCTTGAAAACAAGAATC
5'Sgf73	ATGAGGTCAGGCGATGCAGAGATTA
3'Sgf73	GTGAACATGCTGGATAACGTGCATG
gSGF11a	TGGGATACTGAATAACCTGTTAACCACATTGATCCAGGACATTGTAGCTCGGGAAAATGTGACTGTCGCCCGTACATT
gSGF11b	ACACATCCCTGCCACAATTCTCACAGTGAATATACTGAGAGGACTCTTGTTGCTTCACAAGTTCTTGAAAACAAGAATC
5'Sgf11	GCGTTTCTTCCGTTGAGCAGAGCAG
3'Sgf11	CTGTCTGTGCCTTTTCAATTACCCAT
gSUS1a	CTGACTATTCAGATCACCGTCACATTTATTAGAATTTCAAACGAACTAAAAGCCAGATGTGACTGTCGCCCGTACATT
gSUS1b	CGTTCTCTTTTCAATAAATTTAGTGATAAAATATTCACATACCTAATGCTTTGGGTTCACAAGTTCTTGAAAACAAGAATC
5'Sus1	GGCATGGCTTGACCAACACATGCGACA
3'Sus1	CCGATGAGCATATGTAATAATATTGGGA
5'Rad52	TTACTCATCGCCAAAGAGTCTGCTCTTC
3'Rad52	GTAAATATTAATACGACACATGGAGGAA

Primers used for amplification of G418^r begin with the letter g; primers used to confirm insertion of a gene into the chr. begin with 5 or 3; primers used for amplification of *URA3* begin with the letter p.

Dilution pronging survival assays

To test survival of cells expressing EcoRI, yeast cells were grown on Raff-Ura plates for 1-3 days at 30 °C and harvested into water, diluted 1/50, sonicated for 7 s, and quantitated using a hemocytometer in conjunction with a United Scope model M837T phase contrast microscope (Hopewell Junction, NY). A total of 2 x 10^7 cells were then added to a 96-well microtiter dish with H_2O in a total volume of 220 μL per well and serially diluted 5-fold, followed by pronging to control plates containing 2% Raff-Ura

and selective plates containing 3% Gal-Ura. Cells were grown at 30 °C for 3-4 days and evaluated for sensitivity to EcoRI endonuclease killing. Mutants were classified as resistant to EcoRI (R), moderately sensitive (S) with < 25-fold killing (less than 2 columns of reduced growth relative to wildtype cells), or strongly sensitive (SS) exhibiting ≥ 25-fold killing (≥ 2 full columns of less growth than wildtype cells).

Bleomycin and MMS survival studies were done in a similar way. Mutants were patched to YPDA and grown for 1-2 days at 30 °C. Cells were then harvested, diluted, sonicated, counted, and serially diluted 5-fold in a microtiter dish. The cells were then pronged onto synthetic glucose complete plates with two different final concentrations of bleomycin (2 μg/ml and 4 μg/ml) or YPDA plus MMS (2 mM). Sensitivity was then evaluated after growth at 30 °C for 3-4 days.

Interchromosomal-plasmid recombination efficiency

Plasmid DNA preparation

Plasmid pLKL37Y was digested with BseRI (New England Biolabs, Inc.) to induce a DSB in the *HIS3* gene. A typical digest contained 54 μl pLKL37Y DNA, 326 μl ddH_2O, 100 μl 5X KGB buffer, and 20 μl BseRI (40 units) in a final volume of 500 μl. The reaction mixture was incubated for ≤ 2 h at 37 °C, followed by heat inactivation of the enzyme at 65 °C for 20 min. Samples were then run on a 0.8% agarose gel to verify complete digestion.

Transformation

Forty-eight EcoRI-sensitive mutants (11) were transformed with BseRI-digested pLKL37Y (500 - 1500 ng per transformation) using the higher efficiency protocols of Gietz *et al.* (32) or Tripp *et al.* (33). Recombinant cells with integration of the entire

plasmid into *his3Δ1* became His^+ Ura^+ and were selected for on Glu-His-Ura plates (Glucose complete plates minus histidine and uracil). All mutants were also transformed with uncut vector pRS315 (10 - 50 ng per transformation) and spread to Glu-Leu plates to serve as an internal control for differences in transformation efficiencies among mutants.

Qualitative analysis of intrachromosomal direct repeat recombination

To test intrachromosomal direct repeat recombination efficiency, mutants and WT cells containing the pLKL37Y (*HIS3 URA3*) insertion in chromosome XV were patched onto YPDA plates, grown for 1-2 days at 30 °C, and transferred to fresh YPDA and 5-FOA plates using a velvet-cloth-covered cylinder. The freshly imprinted YPDA plate was immediately used as a new master plate to replica-plate cells to fresh 5-FOA and YPDA plates.

Rate of intrachromosomal direct repeat recombination

Wildtype cells, RAD52 group control mutants, and other mutants were grown overnight in synthetic broth selective for His^+ Ura^+ cells. Then approximately 2.0×10^3 cells were added to non-selective YPDA broth in 7 separate 0.6 ml microfuge tubes and grown for 2 days at 30 °C. The cells were then serial diluted 10-fold (10^{-1}-10^{-4} dilutions) into a 96-well microtiter dish and aliquots were spread to YPDA and 5-FOA plates. After 3-4 days, colonies were counted and the median rate of recombination was determined using the method of the median (36).

Frequency of loss of heterozygosity (LOH)

Diploid strains were prepared by mating both haploid mating types (*MATα* and *MATa*) on YPDA plates. Plates were split into 3 sections; each individual haploid was

patched out into a square either at the top or bottom of the plate and both mutants were patched out and mixed into a square in between both haploid patches. After 1-2 days of growth, the plates were replica plated onto Glu-Leu-Ura-Ade-Trp plates to select for diploids.

Wildtype cells, RAD52 group control mutants, and other mutant diploid cells were harvested from plates depleted of leucine, uracil, adenine, and tryptophan into YPDA broth, diluted 1/50, sonicated for 7 s, and counted using a hemocytometer and phase contrast microscope. A total of 500 cells were then added to YPDA broth and grown for 36 h at 30 °C. The cells were then serial diluted 10-fold and spread to YPDA, 5-FOA, and 5-FOA-Lys (5-FOA minus lysine) or 5-FOA-Met (5-FOA minus methionine) plates. Colonies were then counted after 3-4 days at 30 °C.

CHAPTER III

Results and Discussion

The primary goal of the current project was to further investigate the functions of new *S. cerevisiae* genes in homologous recombination and maintenance of chromosome stability. Bennett *et al.* (20) and Game *et al.* (21) screened diploid yeast deletion libraries for gamma radiation sensitivity. Together, they identified a total of 211 gamma sensitive mutants, 8 of which are part of the DSB repair-deficient RAD52 group (*rad50, rad51, rad52, rad54, rad55, rad57, mre11,* and *xrs2*). Previous graduate students Jennifer Summers, Sunaina Sethi, and Jennifer DeMars utilized *in vivo* EcoRI expression to screen the 201 non-RAD52 group mutants to determine which of them were specifically deficient in repair of DSBs (22–24). Using both *MATα* and *MATa* haploid yeast deletion libraries, they identified 73 non-RAD52 group haploid mutants that exhibited reduced survival after expression of EcoRI. Most of the 73 mutants were also killed by exposure to bleomycin and MMS. Forty-eight of the identified genes are involved in nuclear processes where DNA repair occurs. The results from the EcoRI, MMS, bleomycin, and gamma screens are summarized in Table 2. RAD52 group mutants are located in the top of the table and the 48 others are listed alphabetically in the bottom of the table.

Table 2. Survival of the 48 new mutants after exposure to EcoRI, MMS, bleomycin, and gamma radiation.[b]

Mutant	EcoRI$^{S/R}$		MMS (mM)		bleo (μg/ml)		Γ (krads)		Mutant	EcoRI$^{S/R}$		MMS (mM)		bleo (μg/ml)		Γ (krads)	
	MATα	*MATa*	1	2	2	4	30	60		*MATα*	*MATa*	1	2	2	4	30	60
RAD52 group:																	
rad50	S	S	SS	SS	SS	SS	SS	SS	*rad55*	S	S	SS	SS	R	SS	SS	SS
rad51	S	S	SS	SS	SS	SS	SS	SS	*rad57*	S	R	SS	SS	R	SS	SS	SS
rad52	S	S	SS	SS	SS	SS	SS	SS	*mre11*	S	S	SS	SS	SS	SS	SS	SS
rad54	S	S	SS	SS	SS	SS	SS	SS	*xrs2*	N/D	S	SS	SS	SS	SS	SS	SS
akr1	SS	S	R	R	R	R	R	S	*mms22*	SS	SS	SS	SS	R	S	S	S
apq13/net1[a]	SS	S	S	SS	S	SS	R	R	*mms4*	SS	SS	S	SS	R	R	R	R
arp5	N/D	S	R	S	R	R	R	S	*not5*	SS	SS	R	R	R	R	R	R
bck1	SS	S	S	SS	R	R	R	S	*nup84*	S	SS	R	S	S	SS	R	R
bik1	N/D	S	R	R	R	R	R	R	*och1*	S	N/D	R	S	S	SS	R	R
bud30/rpc53[a]	N/D	SS	R	R	S	S	S	S	*rad5*	S	R	SS	SS	S	SS	R	R
bud32	N/D	S	R	R	SS	SS	S	SS	*rpb9*	S	S	R	SS	S	SS	S	SS
bur2	S	SS	R	S	R	R	R	R	*rtf1*	S	SS	R	S	R	SS	S	SS
cax4	SS	SS	R	R	SS	SS	S	SS	*rtt109 (rem50)*	N/D	SS	R	SS	R	S	R	R
ccr4	N/D	S	R	R	S	SS	R	R	*sae2*	S	S	R	S	R	S	R	S
cdc40	N/D	SS	SS	SS	SS	SS	SS	SS	*sfp1*	SS	S	R	R	R	S	R	R
cgi121	SS	SS	R	R	S	S	SS	SS	*spt10*	S	S	R	S	SS	SS	SS	SS
cnm67	SS	S	R	S	R	SS	S	SS	*spt20*	S	R	R	R	S	SS	R	R
ctf4	SS	SS	SS	SS	R	S	R	R	*taf14*	SS	S	S	SS	R	S	R	R
ctf8	SS	S	S	SS	R	S	R	S	*trm9*	S	SS	S	S	S	S	R	R
dcc1	SS	SS	S	SS	R	S	R	R	*tsr2/ylr434c*[a]	S	S	R	R	R	S	R	S
ddc1	S	S	R	SS	R	R	R	R	*ubp8*	S	SS	R	R	R	R	R	R
eaf1/opi7[a]	S	N/D	R	S	R	S	S	S	*ubr1*	S	N/D	S	S	R	S	SS	SS
exo1	S	S	R	R	R	R	S	S	*ume6*	SS	S	R	R	R	R	R	S
gcn5	SS	S	R	SS	R	S	R	R	*ybr099c*	SS	S	S	SS	R	R	R	R
htl1	SS	SS	R	S	SS	SS	SS	SS	*ydr433w/npl3*[a]	SS	N/D	R	SS	SS	SS	R	R
lrp1	SS	S	R	R	R	S	R	R	*ylr235c/top3*[a]	S	S	SS	SS	R	S	R	S
lsm7	S	SS	S	S	R	S	R	S	*yml009w-b/spt5*[a]	SS	S	S	SS	R	S	R	R
mms2	S	S	S	SS	R	R	R	R	*yml012c-a/ubx2*[a]	S	S	S	SS	R	S	R	R

[a] Gene names separated by a forward slash indicate deletions within two overlapping open reading frames. The coding region of the first gene listed was deleted in these strains.
[b] Mutants were ranked as resistant (R), moderately sensitive (S), strongly sensitive (SS), or not done (N/D) .

The first goal of this project was to determine interchromosomal recombination efficiency of each of the 48 mutants using a plasmid:chromosome recombination assay developed by previous graduate student Rachel Roberts (37). The assay utilized a plasmid (pLKL37Y) that contains two genes, *URA3* and *HIS3*. After a DSB was induced within the *HIS3* gene by the restriction endonuclease BseRI, the broken plasmid was transformed into yeast cells where it could recombine with *his3-Δ*1 on chromosome XV, resulting in integration of the plasmid into the chromosome (Figure 5).

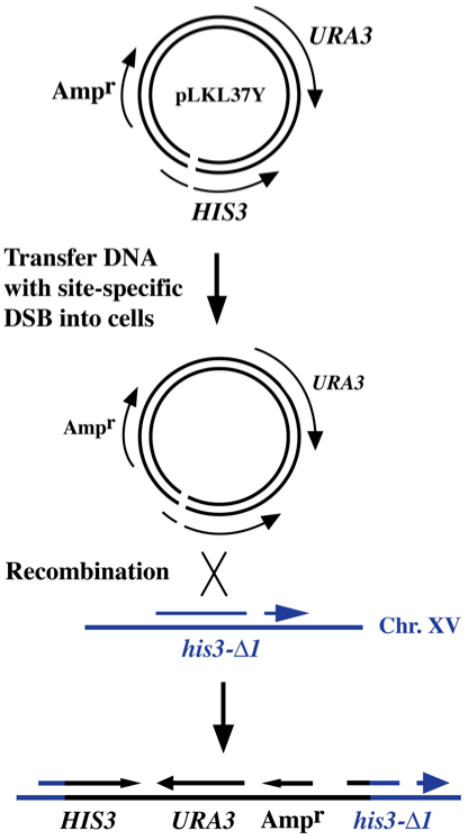

Figure 5. Plasmid recombination assay for repair of a site-specific DSB on a plasmid.

Uncut plasmid pRS315 (*CEN/ARS LEU2*) was simultaneously transformed into the cells along with linearized pLKL37Y to determine total plasmid transformation efficiency. Colony forming units (CFUs) per μg of DNA for pRS315 transformations were calculated based on the number of colonies on glucose complete plates depleted of leucine. Recombinant CFUs per μg of linearized pLKL37Y DNA was calculated from the number of colonies on glucose complete plates depleted of histidine and uracil. The normalized frequency of recombination was then calculated by dividing the recombination efficiencies by the plasmid transformation efficiencies. Mutants were tested up to 3 times, using up to 7 isolates per assay, in an effort to get good statistics and reduced dispersion (low standard deviation). As expected, control *rad57* cells exhibited a

modest decrease in plasmid:chromosome recombination efficiency (14 fold decrease from WT cells). Seven of the mutants displayed reduced interchromosomal recombination (2–3 fold decrease from WT cells), while nine of the mutants had increased recombination compared to WT (2 –10 fold increase from WT cells) (Table 3). Two of the strains, *taf14* and *och1*, displayed 3.4 and 2.6 fold increases compared to WT, respectively, but their standard deviations were overlapping with WT standard deviations, so further testing will need to be done to verify the results. Thus, 16 of the 48 mutants displayed differences from WT. However, most mutants were only moderately changed from WT.

Table 3. Results from the plasmid:chromosome recombination assay of *rad57* and the 48 new mutants.

Strain	% Relative to WT	Fold Change from WT	Strain	% Relative to WT	Fold Change from WT
Wildtype	100.0 ± 34.4%		*rad57*	7.0 ± 1.9%	–14.2x
Nuclease Processing of DNA:			**Transcription Regulation and RNA Modification:**		
exo1	88.7 ± 8.9%	–1.1x	*apq13/net1*[a]	73.6 ± 15.4%	–1.4x
mms4	56.1 ± 7.1%	–1.8x	*bud30/rpc53*[a]	33.5 ± 4.5%	–3.0x
sae2	44.3 ± 4.5%	–2.3x	*bud32*	998.0 ± 325.3%	+10.0x
ybr099c	57.4 ± 5.4%	–1.7x	*bur2*	38.2 ± 1.5%	–2.6x
ylr235c/top3[a]	254.0 ± 52.3%	+2.1x	*ccr4*	295.7 ± 46.1%	+3.0x
			not5	97.0 ± 6.0%	–1.0x
Histone Modification/ Remodeling:			*nup84*	67.7 ± 1.7%	–1.5x
arp5	44.0 ± 14.9%	–2.3x	*rpb9*	46.7 ± 6.5%	–2.1x
eaf1/opi7[a]	89.1 ± 38.8%	–1.1x	*rtf1*	87.8 ± 13.8%	–1.1x
gcn5	62.9 ± 22.3%	–1.6x	*sfp1*	48.8 ± 7.2%	–2.0x
rtt109 (rem50)	93.9 ± 13.7%	–1.1x	*spt20*	905.2 ± 242.8%	+9.1x
spt10	59.1 ± 28.2%	–1.7x	*taf14*	341.6 ± 237.3%	+3.4x
ubp8	81.8 ± 22.5%	–1.2x	*ume6*	134.3 ± 21.2%	+1.3x
			yml009w-b/spt5[a]	74.7 ± 15.7%	–1.3x
Chromosome Stability/ Segregation:			*cdc40*	459.8 ± 112.6%	+4.6x
bik1	44.5 ± 5.6%	–2.2x	*lrp1*	83.8 ± 3.0%	–1.2x
cgi121	36.3 ± 1.6%	–2.8x	*lsm7*	231.4 ± 40.6%	+2.3x
cnm67	68.6 ± 24.2%	–1.5x	*trm9*	46.9 ± 0.9%	–2.1x
ddc1	65.2 ± 10.2%	–1.5x	*tsr2/ylr434c*[a]	66.2 ± 7.6%	–1.5x
mms22	44.5 ± 11.6%	–2.2x	*ydr433w/npl3*[a]	211.6 ± 41.6%	+2.1x
Sister Chromatid Cohesion:			**Post Translational Modification:**		
ctf4	86.2 ± 17.4%	–1.2x	*akr1*	55.2 ± 19.5%	–1.8x
ctf8	143.0 ± 15.7 %	+1.4x	*bck1*	46.9 ± 7.8%	–2.1x
dcc1	94.6 ± 14.1%	–1.1x	*cax4*	127.3 ± 17.9%	+1.3x
htl1	96.8 ± 30.8%	–1.0x	*mms2*	100.0 ± 5.8%	1.0
			och1	257.7 ±153.9%	+2.6x
			rad5	78.7 ± 8.1%	–1.3x
			ubr1	69.9 ± 10.5%	–1.4x
			yml012c-a/ubx2[a]	56.9 ± 6.3%	–1.8x

[a] Gene names separated by a forward slash indicate deletions within two overlapping open reading frames. The coding region of the first gene listed was deleted in these strains.

The 48 mutants produced in the interchromosomal assay were then used to test spontaneous direct repeat intrachromosomal recombination efficiency. Initially, integration of the plasmid caused the cells to contain a direct repeat consisting of *HIS3* and *his3-Δ1* with a *URA3* gene in-between. After intrachromosomal recombination, the cells lose the portion of DNA between the direct repeats and become Ura$^-$ (Figure 6).

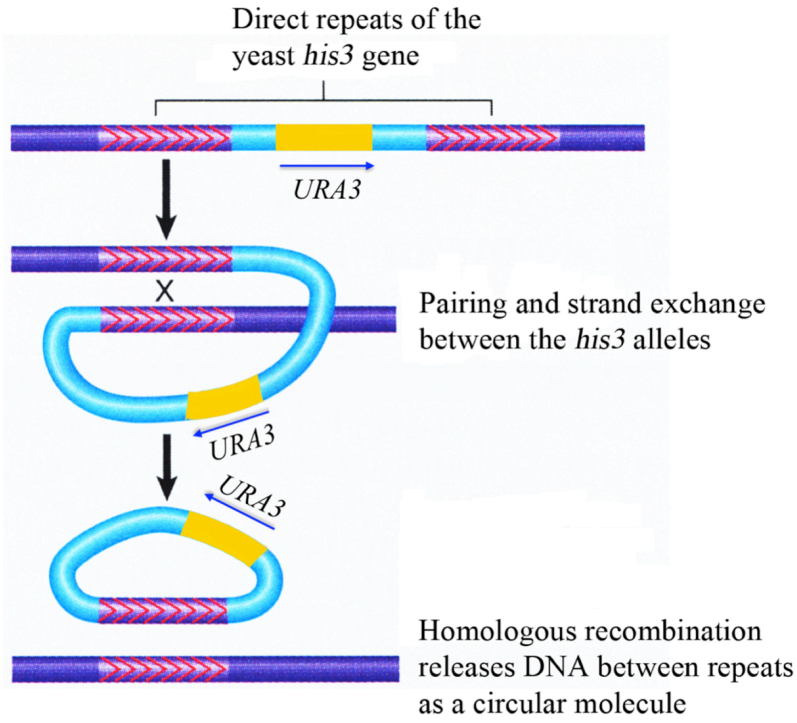

Figure 6. Schematic representation of direct repeat intrachromosomal recombination on chromosome XV. Homologous recombination occurs between the *his3* alleles, releasing the DNA between the two alleles, which contains the *URA3* gene.

A qualitative replica-plating assay was utilized to quickly screen all 48 mutants (Figure 7). This was done by growing square patches of recombinant WT and mutant cells on non-selective YPDA media (a master plate). The master plate was then pressed onto a velvet cloth, creating an imprint of the cells on the velvet. The imprinted cells were then transferred to a new YPDA plate and a 5-fluoroorotic acid (5-FOA) plate. 5-

FOA is toxic to *URA3* cells but not *ura3* mutants due to formation of a toxic byproduct. A double imprint was then performed using the new YPDA plate as the master plate for transfer to another YPDA and 5-FOA plate. Some mutants could be classified using a single replica; for others, double-imprint replicas produced best results.

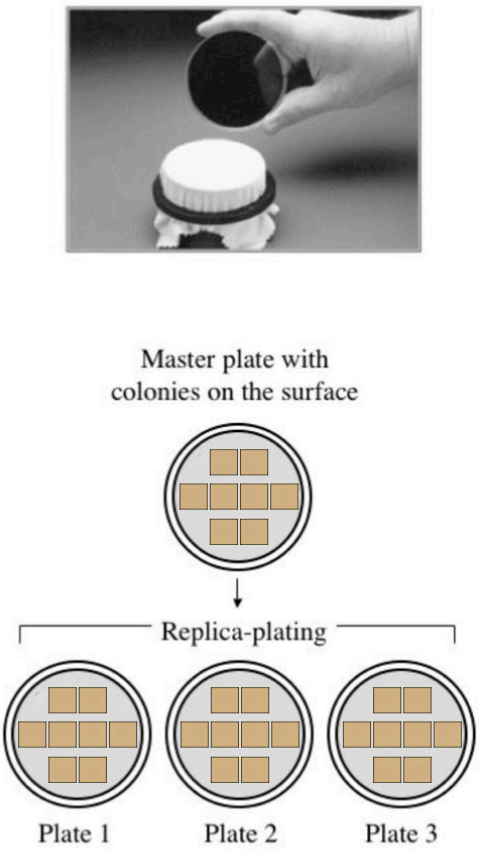

Figure 7. Illustration of replica-plating assay (22). Cells were grown on YPDA and then pressed onto a velvet cloth creating an imprint of the cells that could be transferred to new plates.

The efficiency of this assay was first tested using RAD52 group mutants. Figure 8 shows the results from the test with the control YPDA plate on the left and the 5-FOA double imprint replica plate on the right. As expected, *rad51* and *rad52* (B and E, respectively) exhibited the greatest reduction in intrachromosomal recombination

compared to WT (A). *rad50*, *rad54*, and *rad57* (C, D, and F, respectively) expressed modest decreases compared to WT (Figure 8).

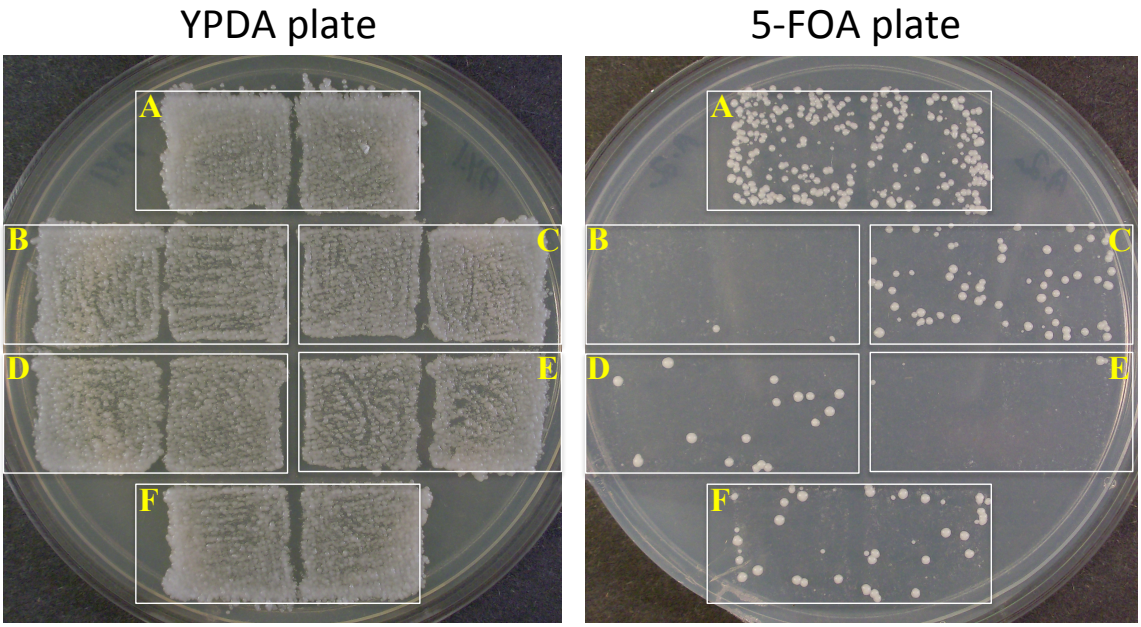

Figure 8. Testing RAD52 group mutants for intrachromosomal recombination efficiency on YPDA (left) and 5-FOA (right) plates. (A) WT; (B) *rad51*; (C) *rad50*; (D) *rad54*; (E) *rad52*; (F) *rad57*.

After growing for 2-3 days at 30 °C, WT cells showed many 5-FOA^r colonies (Figure 9A). In contrast, control *rad52* cells reproducibly produced no or very few 5-FOA^r colonies because intrachromosomal recombination is strongly reduced in these mutants (Figure 9A). The non-RAD52 group mutants were categorized based on sensitivity or resistance to 5-FOA relative to WT cells. Mutants that had fewer colonies on 5-FOA plates compared to wildtype demonstrated reduced intrachromosomal recombination efficiency and were characterized as 5-FOA sensitive (5-FOA^s). Alternatively, mutants that had more colonies on 5-FOA plates compared to WT demonstrated hyper-intrachromosomal recombination and were characterized as 5-FOA resistant (5-FOA^r). Mutants that had similar colony numbers to wildtype were characterized as WT. As shown in Figure 9A and 9B, *not5*, *ume6*, *mms2*, and *ccr4* all

showed fewer colonies relative to WT cells and *ubp8* mutants demonstrated a large increase in 5-FOA^r colonies relative to wildtype.

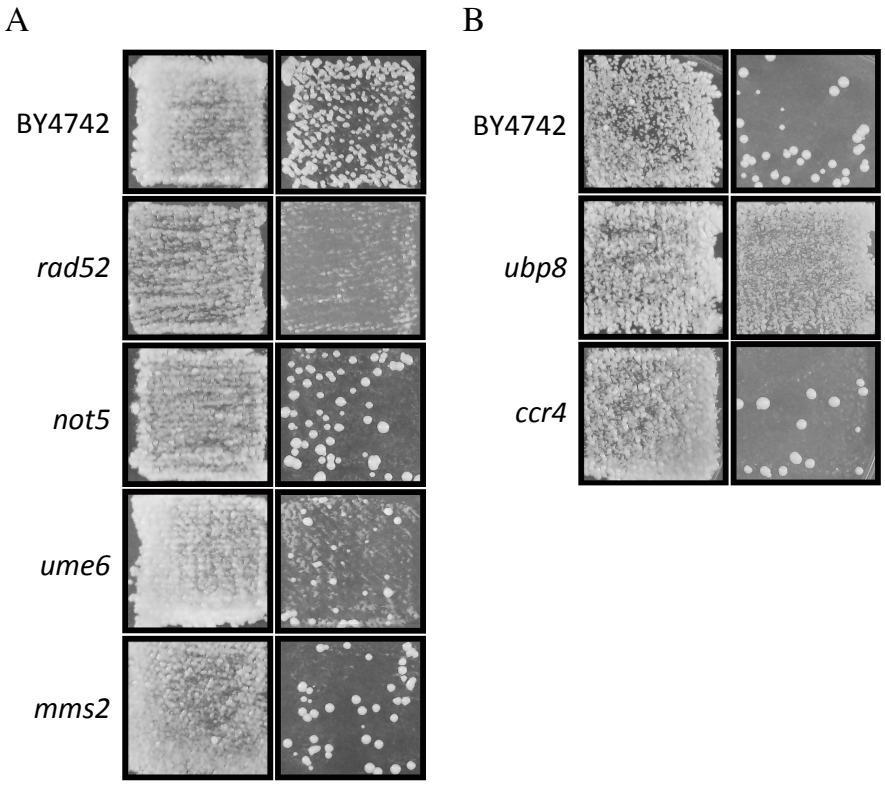

Figure 9. Replica plates of recombinant cells on YPDA (left square) and 5-FOA (right square) plates. (A) Example of single imprint replica plating; (B) Example of double imprint replica plating.

Table 4 shows results from the qualitative intrachromosomal recombination replica-plating assays. Five control RAD52 group mutants and fourteen of the 48 other mutants displayed reduced intrachromosomal recombination and 3 mutants had increased intrachromosomal recombination. Qualitative intrachromosomal recombination efficiencies were not determined (N/D) for two of the mutants because 2 separate isolates of each did not grow on YPDA or 5-FOA plates after replica plating. The remaining 29 mutants produced results similar to wildtype.

Table 4. Results from the qualitative intrachromosomal recombination assay of RAD52 and non-RAD52 group mutants.

Mutant	5-FOA$^{s/r}$	Mutant	5-FOA$^{s/r}$
rad50	5-FOA^{s}	*rad54*	5-FOA^{s}
rad51	5-FOA^{s}	*rad57*	5-FOA^{s}
rad52	5-FOA^{s}		
Nuclease Processing of DNA:		**Transcription Regulation and RNA Modification:**	
exo1	WT	*bud30/rpc53*[a]	5-FOA^{s}
mms4	WT	*ccr4*	5-FOA^{s}
sae2	WT	*not5*	5-FOA^{s}
ybr099c	WT	*rpb9*	5-FOA^{s}
ylr235c/top3[a]	WT	*sfp1*	5-FOA^{s}
		ume6	5-FOA^{s}
Histone Modification/ Remodeling:		*lrp1*	5-FOA^{s}
eaf1/opi7[a]	5-FOA^{s}	*tsr2/ylr434c*[a]	5-FOA^{s}
ubp8	5-FOA^{r}	*spt20*	5-FOA^{r}
arp5	WT	*yml009w-b/spt5*[a]	5-FOA^{r}
gcn5	WT	*apq13/net1*[a]	WT
rtt109 (rem50)	WT	*bud32*	WT
spt10	WT	*bur2*	WT
		nup84	WT
Chromosome Stability/ Segregation:		*rtf1*	WT
mms22	5-FOA^{s}	*taf14*	WT
bik1	WT	*cdc40*	WT
cgi121	WT	*lsm7*	WT
cnm67	WT	*trm9*	WT
ddc1	WT	*ydr433w/npl3*[a,b]	N/D
Sister Chromatid Cohesion:		**Post Translational Modification:**	
ctf4	5-FOA^{s}	*bck1*	5-FOA^{s}
ctf8	WT	*cax4*	5-FOA^{s}
dcc1	WT	*mms2*	5-FOA^{s}
htl1	WT	*akr1*	WT
		rad5	WT
		ubr1	WT
		yml012c-a/ubx2[a]	WT
		och1[b]	N/D

[a] Gene names separated by a forward slash indicate deletions within two overlapping open reading frames. The coding region of the first gene listed was deleted in these strains.
[b] N/D, Not determined due to growth defects on YPDA and 5-FOA plates.

The 14 strains that displayed reduced levels and the 3 that displayed increased levels of intrachromosomal recombination in the qualitative assay, as well as the 2 mutants that could not be tested by this technique, were retested using a more quantitative assay with *rad51*, *rad52*, and *rad57* control mutants. The recombinant cells were grown for 1 day at 30 °C in synthetic broth depleted of histidine and uracil, diluted down to ~1 x 10^4 cells/ml in YPDA broth, and incubated at 30 °C for ~12 generations (24 h). The cells were then serially diluted 10 fold and spread to YPDA and 5-FOA plates. After 3-4 days of incubation at 30 °C, colonies were counted and the frequency of loss of *URA3* was calculated using the method of the median (36). Fourteen of the mutants were found to affect spontaneous intrachromosomal recombination and are shown in Table 5. Interestingly, *ubp8* reproducibly displayed ~600 fold increase in intrachromosomal recombination compared to WT. Two other mutants, *mms22* and *bud30/rpc53*, showed stronger decreases (90 and 130 fold, respectively) than RAD52 group controls (81 and 65 fold for *rad51* and *rad52*, respectively).

Table 5. Results from the quantitative intrachromosomal recombination assay of RAD52 and non-RAD52 group mutants.

Mutant	Recombination rate (x 10^{-5}) (Conf. int.)	Fold change
WT	12.10 (10.15 – 14.23)	
rad51	0.15 (0.12 – 0.22)	–81.4x
rad52	0.19 (0.10 – 0.24)	–64.6x
rad57	2.53 (1.93 – 2.92)	–4.8x
Histone Modification/ Remodeling:		
eaf1/opi7[a]	0.50 (0.35 – 1.67)	–24.3x
ubp8	6777.20 (6564 – 8846)	+560.1x
Chromosome Stability/ Segregation:		
mms22	0.13 (0.04 – 0.24)	–90.4x
Sister Chromatid Cohesion:		
ctf4	1.70 (0.55 – 3.16)	–7.1x
Transcription Regulation and RNA Modification:		
bud30/rpc53[a]	0.09 (0.02 – 0.41)	–135.1x
ccr4	0.38 (0.18 – 0.98)	–31.7x
not5	1.20 (0.47 – 1.70)	–10.1x
rpb9	4.45 (0.81 – 10.50)	–2.7x
sfp1	5.88 (5.08 – 14.30)	–2.1x
spt20	9.88 (7.31 – 22.27)	–1.2x
ume6	0.47 (0.13 – 1.13)	–25.5x
yml009w-b/spt5[a]	21.80 (7.34 – 133)	+1.8x
lrp1	1.29 (0.66 – 3.73)	–9.4x
tsr2/ylr434c[a]	4.04 (1.83 – 28.77)	–3.0x
Post Translational Modification:		
bck1	18.94 (12.85 – 64.89)	+1.6x
mms2	0.42 (0.13 – 1.98)	–29.0x
och1[b]	227.00 (N/D)	+18.8x

[a]Gene names separated by a forward slash indicate deletions within two overlapping open reading frames. The coding region of the first gene listed was deleted in these strains.
[b]This is a minimum approximation because of the low number of colonies observed with *och1* cells.
Conf. int., 95% confidence interval.

Library mutants often contain uncharacterized spontaneous secondary mutations in other genes that affect certain phenotypes being tested (11). These secondary mutations are unique to one type of deletion library strain, i.e., if a mutant in a *MATα* library contains a secondary mutation, then the *MATa* library strain will not have that

same secondary mutation. To determine if the surprising results from the *MATα ubp8* recombination assays were real or due to a secondary mutation, linear pLKL37Y was integrated into a *MATa ubp8* library mutant (opposite mating type) and it was tested qualitatively and quantitatively for intrachromosomal recombination efficiency. The qualitative assay displayed a near wildtype phenotype for the *MATa* library strain and the quantitative recombination rate was ~2 fold lower than the wildtype control. Thus, both *MATα* and *MATa ubp8* mutants were EcoRI^s, but only the *MATα* strain exhibited ~600x higher recombination between direct repeats, suggesting that this strain had a secondary mutation providing the hyper-rec phenotype.

With the gamma radiation and EcoRI sensitivity phenotypes seen in both library *ubp8* mutants, it is likely that Ubp8 contributes to chromosome stability in some way. The Ubp8 protein contains the active site for the deubiquitination module (DUBm) within the SAGA (Spt-Ada-Gcn5-Acetyltransferase) acetylation complex and mediates deubiquitination of histone H2B along with Sgf73, Sgf11, and Sus1 (25, 26). The DUBm complex is required for deubiquitination of histone H2B during transcription elongation. Even though Ubp8 contains the enzymatic core for deubiquitination of H2B, it is not active unless all four proteins are in a complex with each other (25, 38).

Out of these four *S. cerevisiae* genes, only one has previously been linked to DNA repair, *SGF11*, which was found to produce sensitivity to bleomycin and MMS (39). To investigate this further, haploid *MATα* library mutants (*sgf73*, *sgf11*, and *sus1*) were tested for sensitivity to EcoRI (Figure 10) and for spontaneous intrachromosomal recombination levels using both qualitative and quantitative assays.

As seen in Figure 10, EcoRI expression had no effect on *sus1*, but *sgf11* displayed a moderate reduction in cell growth and *sgf73* was strongly sensitive. Table 6 shows the results from the quantitative intrachromosomal recombination assays for the *sgf73*, *sgf11*, and *sus1 MATα* library mutants. Similar to the EcoRI survival assays, *sgf11* and *sus1* had wildtype phenotypes, but *sgf73* had a substantial reduction in intrachromosomal recombination efficiency (21-fold).

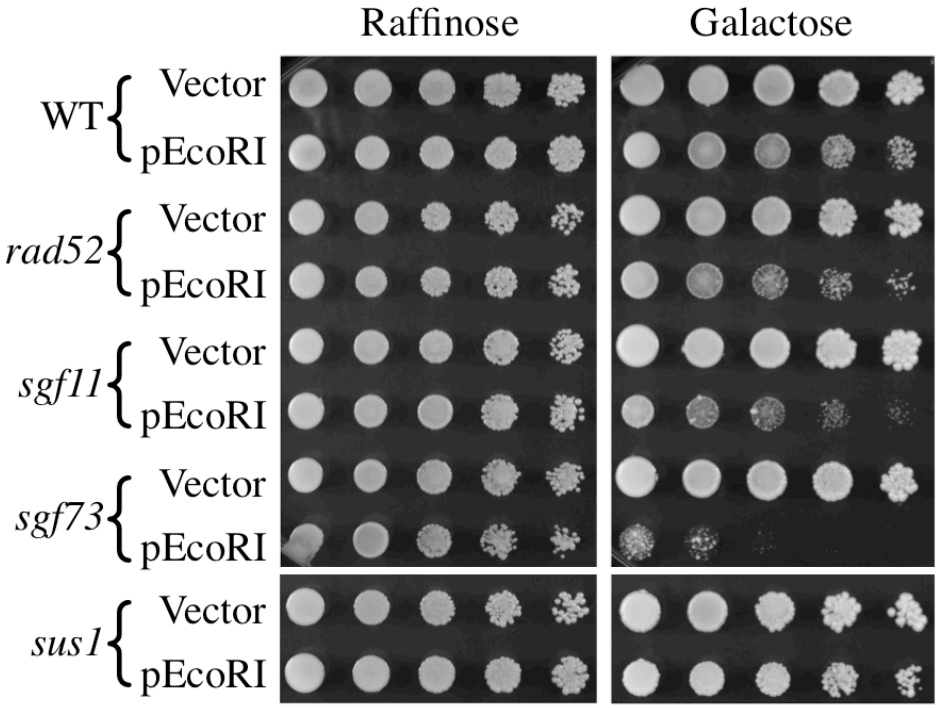

Figure 10. Survival of haploid library *sgf11*, *sgf73*, and *sus1* mutants after induction of EcoRI expression. Cells were serially diluted 5-fold and pronged onto plates.

Table 6. Rates of intrachromosomal recombination for library *MATα* DUBm mutants.

Mutant	Recombination rate (x 10^{-5})	Fold decrease
Wildtype	12.14	
sgf73	0.57	21.2x
sgf11	9.55	1.3x
sus1	8.49	1.4x

The next goal of this project was to construct new *ubp8*, *sgf73*, *sgf11*, and *sus1* mutants using PCR-mediated gene disruption from both *MATa* (BY4741) and *MATα* (BY4742) cells to eliminate potential effects caused by secondary mutations in the library strains. This was done by first PCR amplifying the G418^r gene from the plasmid pFA6MX4 using primers that contain homologous sequences (~56 bp) on the ends to each desired gene. Each PCR product was then subjected to agarose gel electrophoresis to confirm the proper sized fragment was obtained (Figure 11).

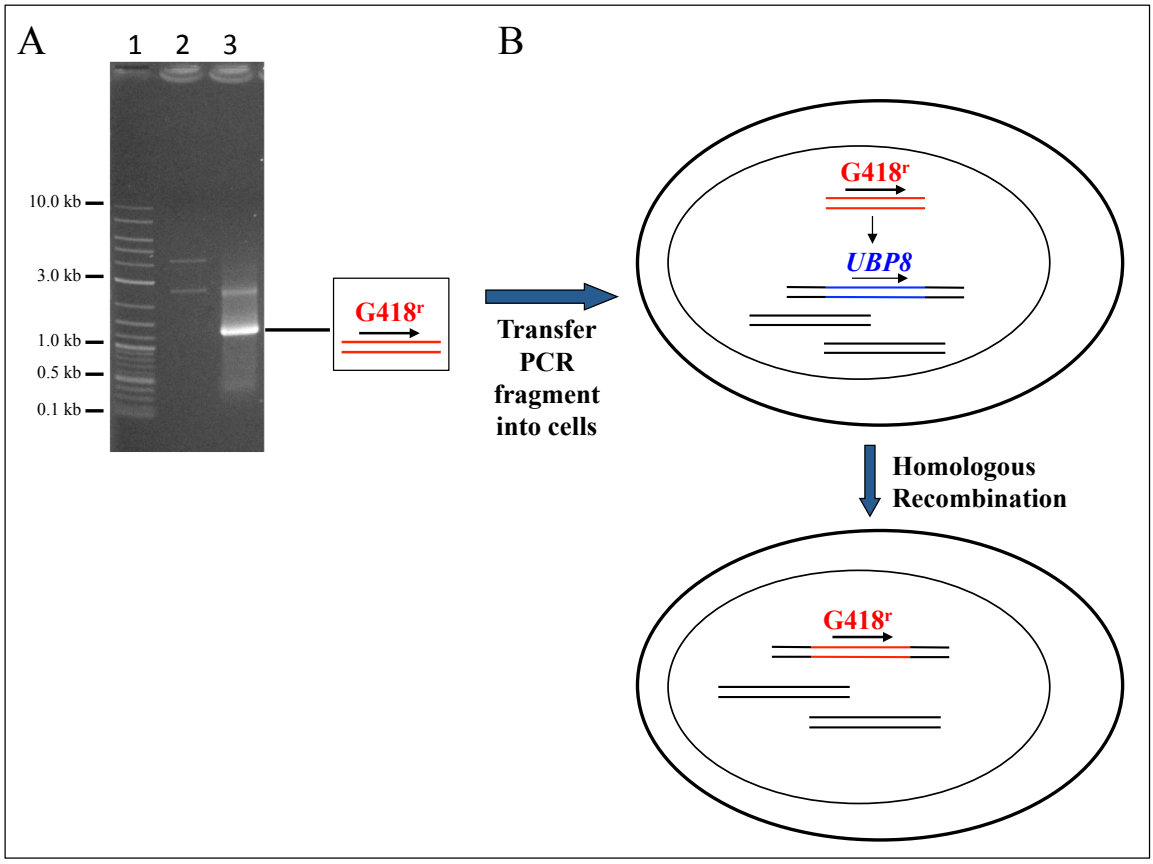

Figure 11. Example PCR amplification of the G418^r gene (~1.2 kb) using *ubp8* primers gubp8a and gubp8b. (A) Lane 1, 2-log DNA ladders; Lane 2, pFA6MX4 plasmid; Lane 3, G418^r gene PCR with *ubp8* primers. DNA was run on a 0.8% agarose gel in 1X TAE at ~140 V; (B) Illustration of *UBP8* gene deletion.

After confirming correct PCR amplification of the G418^r gene, the PCR fragments were transformed into yeast cells using an early stationary phase transformation protocol (31), spread to YPDA plates, incubated for one day and then transferred to YPDA plates supplemented with G418 using replica plating. The colonies that formed on the G418-supplemented plates were then streak purified on a new YPDA+G418 plate to eliminate the possibility of selecting G418^s cells. Chromosomal DNA was then purified from colonies and the gene knockouts were confirmed using PCR amplification with primers that anneal to the outside of the ORF (5' and 3' test primers). Sizes were compared to WT gene PCR fragments using agarose gel electrophoresis. The first attempt at knocking out *ubp8* is shown in Figure 12. A total of 15 independent isolates were PCR amplified from G418^r colonies and all 15 contained wildtype PCR fragments. The cause of this failure is unknown but may be due to the fact that homologous recombination is not as active in early stationary phase cells (40).

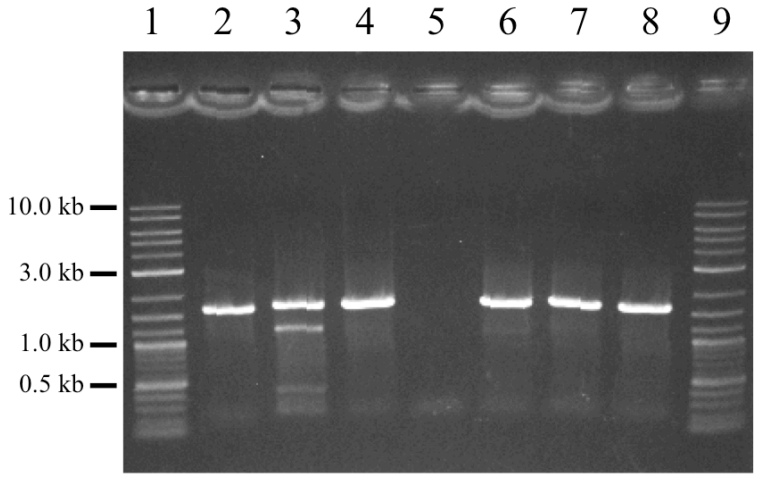

Figure 12. Agarose gel electrophoresis of PCR fragments from G418^r genomic DNA. Lane 1, 2-log ladder; Lanes 2-3, wildtype PCR fragment using *ubp8* test primers; Lanes 4-8, PCR fragments from G418^r genomic DNA amplification using *ubp8* test primers. Fragments were run on a 1% agarose gel.

Correct *ubp8* gene knockouts were finally obtained using the same procedure as before with the exception of the transformation protocol, which was changed to a high efficiency log phase cell transformation method (32, 33). Each DUBm mutant was created using WT cells of both mating types, as well as a *MATα* WT strain with the plasmid pLKL37Y inserted into chromosome XV. Examples of the PCR fragments obtained for *ubp8*, *sgf73*, *sgf11*, and *sus1* are shown in Figure 13. In each case, the WT PCR product is shown on the left and a mutant product on the right. At least 2 independent isolates were obtained and PCR confirmed for each type of mutant that was created.

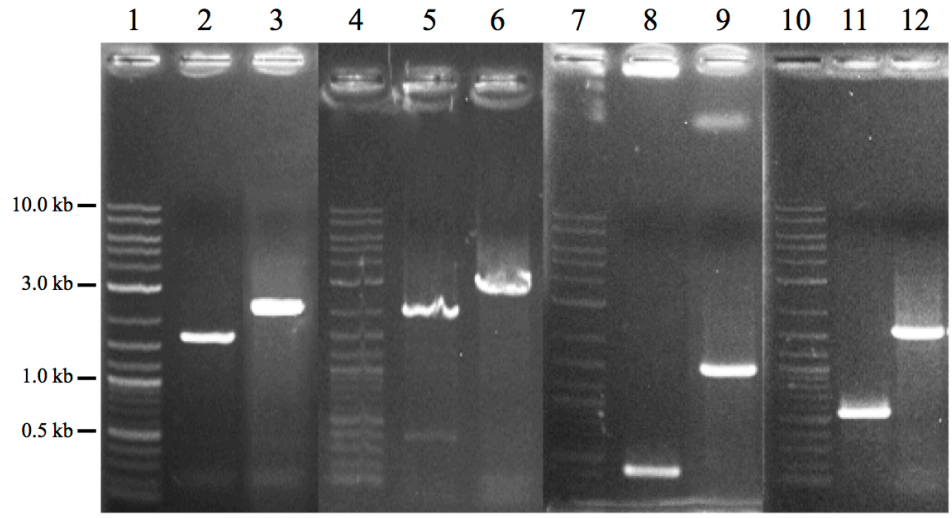

Figure 13. PCR confirmation of DUBm gene knockouts. Lanes 1, 4, 7, and 10 are 2-log DNA ladders; Lanes 2, 5, 8, and 11 are WT PCR fragments using test primers; Lanes 3, 6, 9, and 12 are *ubp8*, *sgf73*, *sgf11*, and *sus1* mutants, respectively.

EcoRI, MMS, and bleomycin survival assays were conducted on the new mutants after confirming successful gene disruption. The EcoRI pronging results for all four DUBm mutants are shown in Figure 14 with *MATα* mutants in section A and *MATa* mutants in section B. As expected, both mating types of each mutant displayed similar

phenotypes. *ubp8* and *sgf73* cells demonstrated EcoRI sensitivity (producing smaller and fewer colonies than WT cells), with *sgf73* being strongly sensitive. These results confirm that the EcoRI sensitivities displayed in *ubp8* and *sgf73 MATα* library mutants are due to the respective gene knockouts and not from secondary mutations. *sgf11* and *sus1* also displayed the same phenotypes as the *MATα* library mutants. These include a moderate reduction in cell growth but not a decrease in survival for *sgf11* and EcoRI resistance for *sus1* cells.

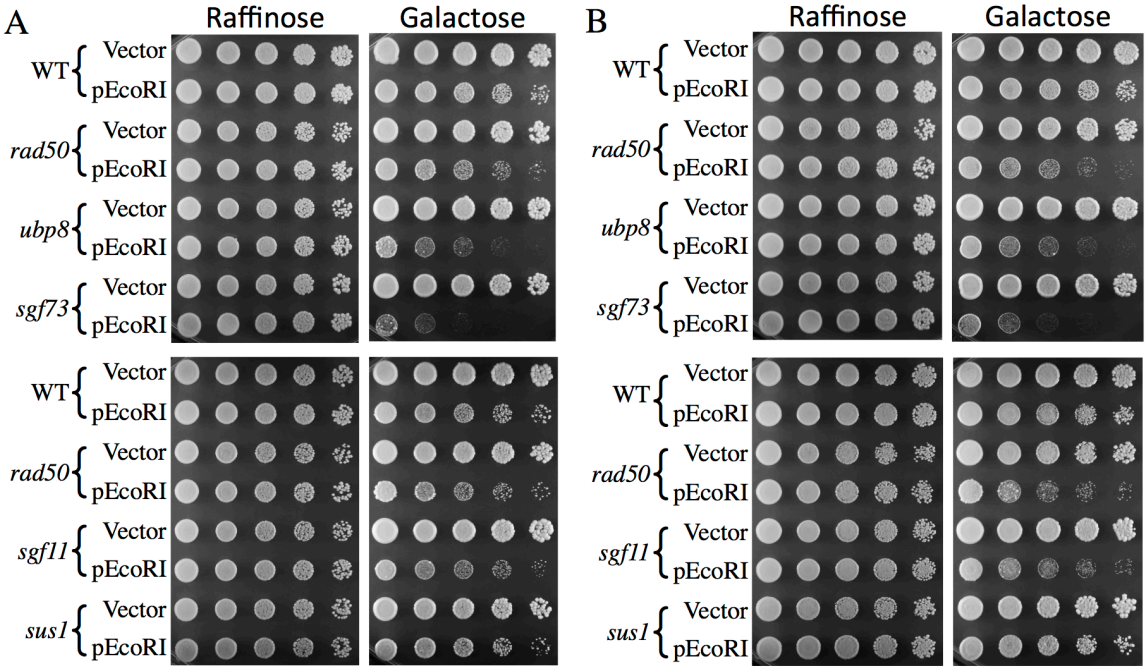

Figure 14. Survival of DUBm mutants after EcoRI expression *in vivo*. (A) *MATα* and (B) *MATa* mutants constructed in this study.

Bleomycin survival results are shown in Figure 15. Mutants were pronged onto YPDA plates as a control and onto glucose synthetic media supplemented with 2 μg/ml and 4 μg/ml bleomycin. Both mating types of each mutant displayed similar results. All mutants were resistant to the lower dose (2 μg/ml) with the exception of the control

mutant, *rad52*, which was strongly sensitive. Interestingly, only *sus1* cells exhibited consistent moderate sensitivity with 4 μg/ml bleomycin. The new *ubp8* mutants were each resistant to bleomycin, which were the same phenotypes observed in the library mutants (11). *sgf11* cells created here were resistant to 4 μg/ml bleomycin. These results differ from those of Kapitzky *et al*. 2010 (39).

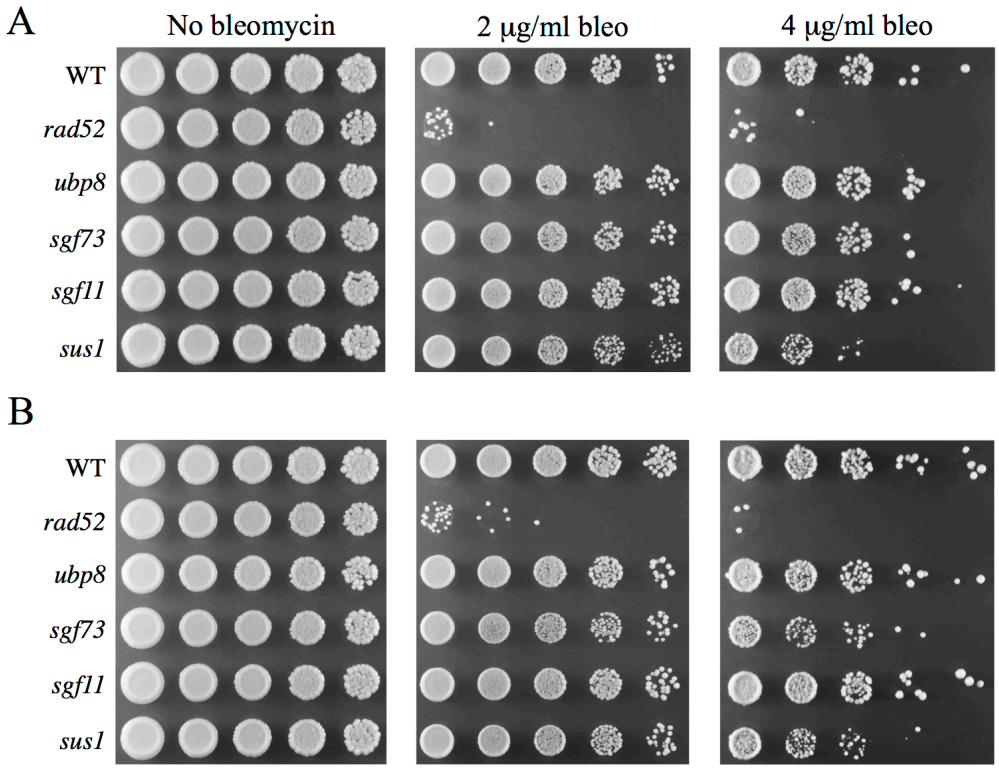

Figure 15. Pronging of DUBm mutants to measure sensitivity to 2 and 4 μg/ml bleomycin. (A) *MAT*α and (B) *MATa* mutants constructed in this study. YPDA plates were used as control plates and bleomycin plates were made with synthetic media.

None of the DUBm mutants displayed sensitivity to 2 μg/ml MMS (Figure 16). Kastenmayer *et al.* (41) previously tested *sus1* haploids for MMS and bleomycin sensitivity. They found that *sus1* cells were sensitive to 1.8 mM MMS but not sensitive to 10 mU/ml bleomycin. It is not clear if the differences seen in *sus1* mutants in this study

and that of Kastenmayer *et al.* are due to differences in the strain background, potencies of the drugs, or some other difference. Results of all survival tests are summarized in Table 7.

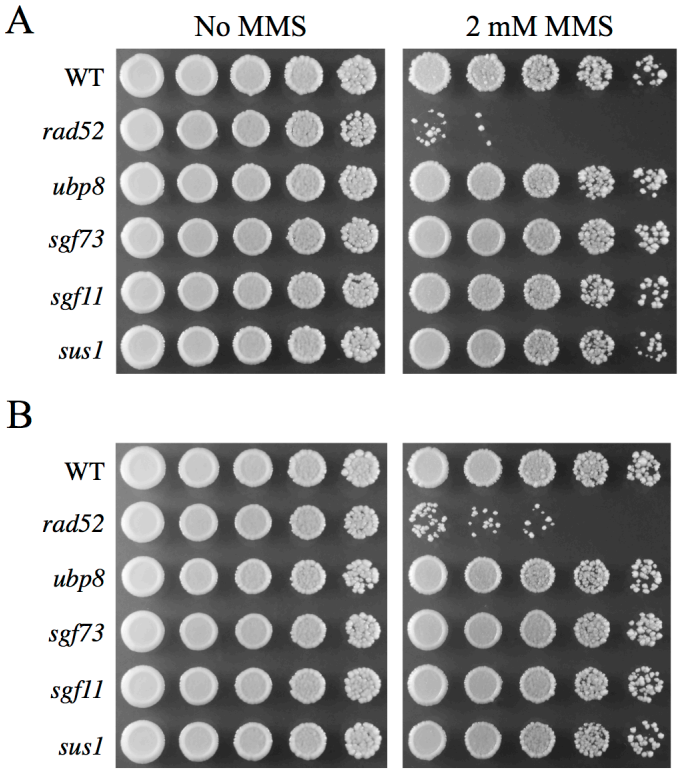

Figure 16. Pronging assays showing that MMS has no effect on DUBm mutants that were constructed in this study. (A) *MATα* cells and (B) *MATa* cells.

Table 7. EcoRI, MMS, and bleomycin sensitivity results for DUBm mutants created using PCR-mediated gene disruption.

Mutant	EcoRI		MMS		bleomycin			
			(2 mM)		(2 μg/ml)		(4 μg/ml)	
	MATα	*MATa*	*MATα*	*MATa*	*MATα*	*MATa*	*MATα*	*MATa*
ubp8	S	S	R	R	R	R	R	R
sgf73	SS	SS	R	R	R	R	R	R
sgf11	R	R	R	R	R	R	R	R
sus1	R	R	R	R	R	R	S	S

Mutants were ranked as resistant (R), moderately sensitive (S), strongly sensitive (SS), or not done (N/D) .

The final goal of this project was to design and test an assay to analyze genome instability through loss of heterozygosity (LOH) in diploid mutants. LOH events arise when diploid cells that are, e.g., *URA3* / *ura3* become *ura3* / *ura3*, going from heterozygous to homozygous at one locus. These events include chromosome loss, chromosome arm loss, allelic crossing over, local gene conversion, and mutation. Nearly half of all LOH events that occur in WT diploid cells are due to homologous recombination, while most of the other half occur from spontaneous loss of a chromosome (42, 43). Almost all LOH events in homologous recombination-deficient RAD52 group mutants occur from loss of a chromosome (42, 43).

Four LOH assays were created to take advantage of auxotrophic markers already present on chromosomes II and XII in *MATα* and *MATa* library mutants, which only require a single additional gene modification to create a useful LOH assay system. Library *MATα* cells (BY4742) and *MATa* cells (BY4741) are each *ura3*, *leu2*, and *his3Δ1*, but only the *MATα* strain is *lys2* and only the *MATa* strain is *met17*. Thus, *α/a* diploids are *ura3 / ura3 leu2 / leu2 his3Δ1 / his3Δ1 lys2 / LYS2 MET17 / met17* and therefore have 2 loci that are naturally heterozygous.

In the first assay system called pBoi1, *URA3* PCR fragments were transformed into *MATa* cells and inserted into chromosome II between *BOI1* and *CDC27*, which is located across the centromere from *LYS2* (Figure 17B). The resulting cells are *LYS2 / lys2 URA3 / (ura3)*. Spontaneous LOH can be monitored by growing the cells in YPDA media and then spreading to 5-FOA plates, which select for cells that have become Ura$^-$. The Ura$^-$ cells can then be tested to see which ones have also lost the *LYS2* marker, which would imply loss of the whole chromosome. The second system, called pTyr1, also

utilized chromosome II, but the *URA3* PCR primers were designed to knock out *TYR1* on the same side of the centromere as *LYS2* (Figure 17A). In the next system, *URA3* was inserted between *EMC6* and *PUF3* on chromosome XII of *MATα* cells, across the centromere from *MET17*, and was called pEmc6 (Figure 17D). The fourth approach also utilized chromosome XII, but *URA3* PCR products were designed to knock out *GAL2* between *MET17* and the centromere. This assay was called pGal2. A schematic representation of each assay is shown in Figure 17.

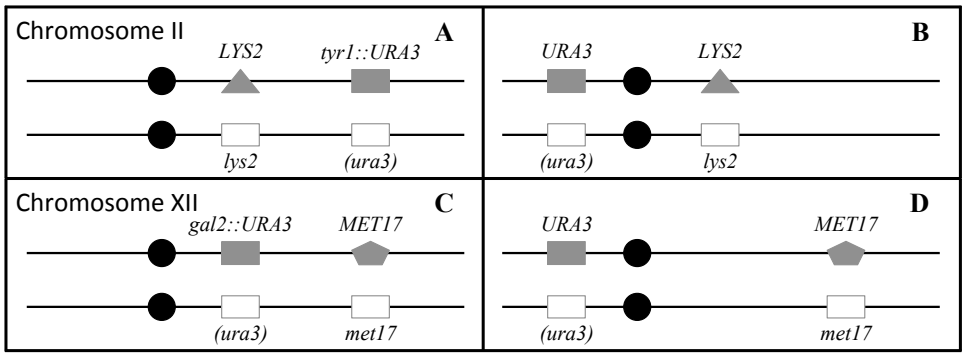

Figure 17. Schematic representation of LOH assays. (A) *TYR1* was knocked out and replaced with *URA3*. (B) *URA3* was inserted between *BOI1* and *CDC27*. (C) *GAL2* was knocked out by insertion of *URA3*. (D) *URA3* was inserted between *EMC6* and *PUF3*.

Plasmid pRS306 (*URA3*) was used for PCR amplification of *URA3* with different primer sets and the PCR products were confirmed using gel electrophoresis (Figure 18A). Each PCR product was then transformed into either *MATα* or *MATa* WT cells using the early stationary phase transformation method and spread to glucose complete plates depleted of uracil to select for Ura^+ cells. Genomic DNA was then purified from the resulting colonies and used to determine correct insertion of *URA3* using PCR with 5' and 3' test primers specific for each assay. Examples of the genomic DNA PCR tests are shown in Figure 18B.

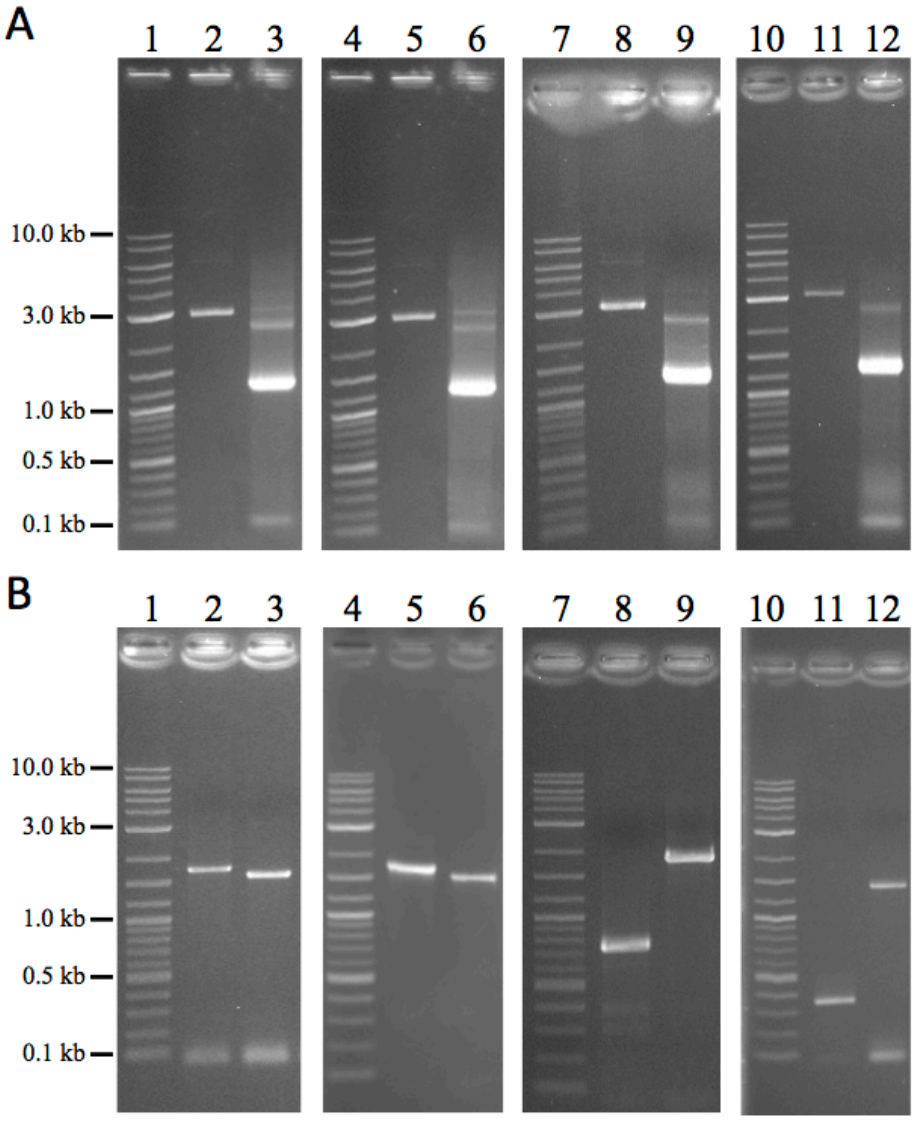

Figure 18. PCR amplification of *URA3* from plasmid DNA and confirmation of *URA3* insertion into genomic DNA. (A) Plasmid PCR; lanes 1, 4, 7, and 10 are 2-log DNA ladders; lanes 2, 5, 8, and 11 are plasmid pRS306; lanes 3, 6, 9, and 12 are *URA3* fragments synthesized with pGal2, pTyr1, pEmc6, and pBoi1 primers, respectively. (B) Chromosome test PCR; lanes 1, 4, 7, and 10 are 2-log DNA ladders; lanes 2, 5, 8, and 11 are products from WT chromosomal DNA using pGal2, pTyr1, pEmc6, and pBoi1 test primers, respectively; lanes 3, 6, 9, and 12 indicate correct insertion of *URA3* using pGal2, pTyr1, pEmc6, and pBoi1 test primers.

Diploid cells were created by separately mating either Ura^+ pTyr1 or pBoi1 *MATa* cells with Ura^- *MATα* cells (BY4742) and Ura^+ pGal2 or pEmc6 *MATα* cells with Ura^- *MATa* cells (BY4741). The resulting diploids were then spread to YPDA and 5-FOA

plates to counterselect for the loss of *URA3*. pTyr1 and pBoi1 diploid cell-derived colonies that formed on 5-FOA plates were then patched to YPDA and glucose complete minus lysine plates to identify isolates that had lost both *URA3* and *LYS2*. 5-FOA^r pGal2 and pEmc6 diploid colonies were patched to YPDA and glucose complete minus methionine plates to detect cells that had lost both *URA3* and *MET17*.

This patching method produced undesired and inconsistent results in all four diploid strains that were tested. LOH events causing the 5-FOA^r phenotype produced results that suggested either all loss of chromosome or no loss of chromosome, which is not consistent with past studies (44). The protocol was adjusted to try to resolve the problem. Cells grown in YPDA broth were simultaneously spread to YPDA plates, 5-FOA plates, and 5-FOA plates minus methionine or lysine. The frequency of chromosome loss (5-FOA^r Met$^-$ or 5-FOA^r Lys$^-$) was calculated by subtracting the frequency of 5-FOA^r Met$^+$ (or 5-FOA^r Lys$^+$) cells from the frequency of total 5-FOA^r cells (representing total LOH events occurring from all possible causes). The results obtained with this adjusted approach suggest that ~60% of LOH events on chromosome XII were chromosome loss (frequency: 127.0 x 10^{-7}), while ~20% of events on chromosome II were from chromosome loss (frequency: 67.5 x 10^{-7}). Kumaran *et al.* (44) previously observed chromosome loss frequencies of 58.0 x 10^{-7} for chromosome XII and 6.0 x 10^{-7} for chromosome II. Possible differences between the results obtained in this study and those of Kumaran *et al.* might be because the current study utilized *MET17* and *LYS2*, which are loci previously reported to have elevated LOH frequencies, no matter what mutant strain is used (45).

Since having more markers on each chromosome improves LOH analysis, a previously published LOH assay system obtained from Yoshida *et al.* was also tested (42). The strains obtained from Yoshida contain 3 wild-type gene markers (*LEU2*, *URA3*, *ADE2*) on chromosome III in *MATa* cells and the corresponding mutant alleles *leu2*, *ura3*, and *ade2* on the same chromosome in *MATα* cells. A schematic representation of the assay performed after the *MATα* and *MATa* cells are mated is shown in Figure 19.

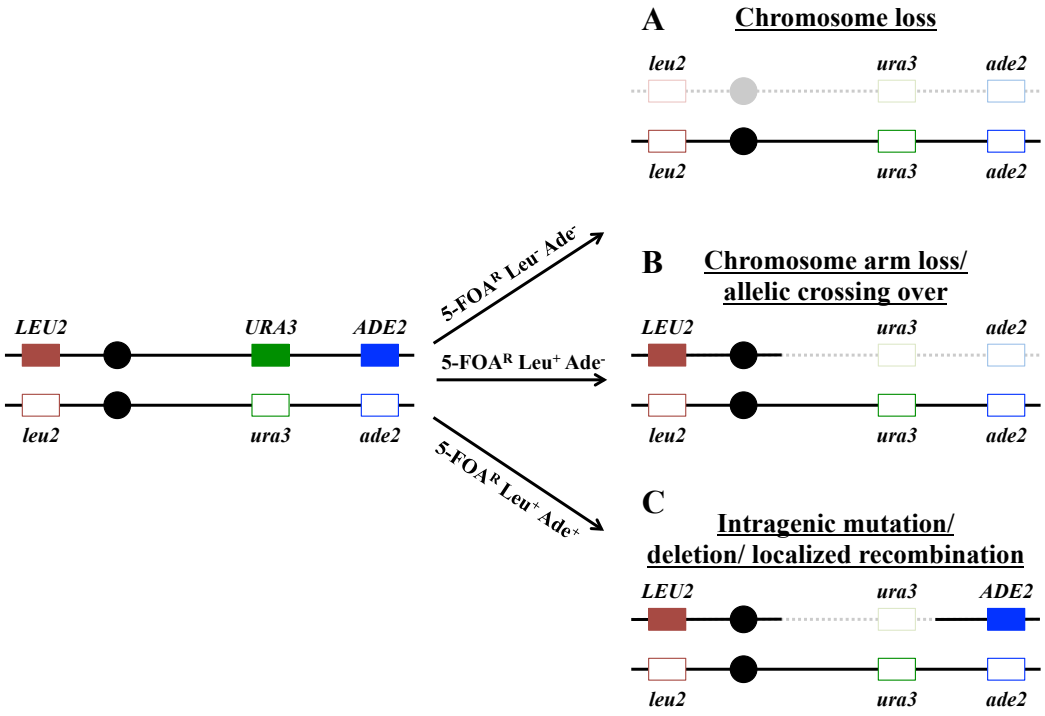

Figure 19. Schematic representation of loss of heterozygosity events on chromosome III.

The protocol used for this assay was similar to the previous LOH assays, with a couple of exceptions. New mutants were made in the new strains using the same procedure used earlier involving insertion of a G418 resistance gene. The mutants that were made consisted of a *rad52* control mutant, *ubp8*, *sgf73*, *sgf11*, and *sus1* cells. All

five were constructed in both *MATα* and *MATa* cells. After creating the diploid strains, they were incubated for 36 h (~18 generations) in YPDA broth, diluted, and then spread to YPDA, 5-FOA, 5-FOA minus leucine, and 5-FOA minus leucine and adenine plates.

The results for these LOH assays are shown in Table 8. In WT cells, 40.4% of the LOH events were due to chromosome loss (forming 5-FOA^r Leu$^-$ cells that have lost markers on opposite sides of the centromere), while ~60% of the events occurred primarily because of homologous recombination, with a smaller number of 5-FOA^r cells formed in other ways such as simple mutation of *URA3* to *ura3*. Results observed here compare favorably with Yoshida *et al.* (42) where they observed a 28 fold increase in total 5-FOA^r cells in *rad52* mutants relative to WT cells, while a 40 fold increase was observed in *rad52* cells in the current study. As expected, recombination-deficient *rad52* cells exhibited much higher levels of chromosome loss (5-FOA^r Leu$^-$) than WT cells (579×10^{-5} vs. 6.1×10^{-5}). Both *sgf73* and *sus1* cells displayed increased chromosome loss (66–73% of all events vs. 40% for WT), while *ubp8* and *sgf11* cells displayed chromosome loss frequencies similar to WT cells.

Table 8. Median frequencies of 5-FOA^r, 5-FOA^r Leu$^-$, 5-FOA^r Leu$^+$ Ade$^-$, and 5-FOA^r Leu$^+$ Ade$^+$ cells.

		Estimated frequency X 10^{-5} (class distribution, %)					
Class[a]	**Phenotype**	**Wild-type**	***rad52***[b]	***ubp8***	***sgf73***	***sgf11***	***sus1***
Total	5-FOA^r	15.2 (100)	582 (100)	8.4 (100)	12.2 (100)	9.7 (100)	25.3 (100)
A	5-FOA^r Leu$^-$	6.1 (40.4)	579 (99.5)	4.2 (50.6)	8.9 (73.0)	5.4 (55.5)	16.8 (66.3)
B	5-FOA^r Leu$^+$ Ade$^-$	8.5 (56.2)	2.8 (0.4)	3.7 (44.7)	3.0 (24.3)	4.0 (41.2)	8.0 (31.6)
C	5-FOA^r Leu$^+$ Ade$^+$	0.52 (3.4)	0.31 (0.1)	0.39 (4.7)	0.32 (2.6)	0.32 (3.3)	0.52 (2.1)

[a] Classification of 5-FOA^r cells together with their phenotypes is shown in Figure 19.
[b] This is a minimum approximation because of the low number of colonies observed with *rad52* cells.

CHAPTER IV

Summary and Conclusions

Two previous studies identified 211 gamma sensitive yeast mutants, 8 of which are part of the RAD52 group. Gamma radiation causes other DNA lesions besides double-strand breaks, so to detect DSB repair genes, these 211 gamma sensitive mutants were screened for sensitivity to *in vivo* expression of EcoRI endonuclease. Of the 211 mutants, 73 were killed when EcoRI was expressed and most of the 73 were also sensitive to the DNA damaging agents bleomycin and methyl methanesulfonate (MMS). Forty-eight of the new genes are involved in nuclear processes, where DNA repair occurs.

The first goal of this project was to utilize a plasmid:chromosome recombination assay developed by previous graduate student Rachel Roberts to determine interchromosomal recombination efficiency in the 48 new mutants. Seven of the mutants displayed modest reduction in plasmid:chromosome recombination compared to WT cells, while nine exhibited increased interchromosomal recombination compared to WT cells (Table 3).

The second goal of this project was to determine spontaneous direct repeat intrachromosomal recombination efficiency of the 48 mutants. The mutants produced in the interchromosomal recombination assay, which contain a direct repeat consisting of *HIS3* and *his3-Δ1* with *URA3* in between, were used in this assay. After intrachromosomal recombination, the cells lose the portion of DNA between the direct repeats and become Ura^-, which can be counterselected for on 5-FOA plates. It was

found that two of the 48 mutants (*ubp8* and *och1*) displayed an increase in spontaneous intrachromosomal recombination (560 and 19 fold increase compared to WT). Twelve mutants displayed between 2 and 135 fold reduction in intrachromosomal recombination compared to WT. Two of the mutants, *bud30/rpc53* and *mms22*, displayed larger decreases (135 and 90 fold, respectively) in intrachromosomal recombination than *rad51* and *rad52* (81 and 65 fold decrease, respectively) (Table 5).

To determine if the 560x increase in intrachromosomal recombination for *ubp8* cells was real or due to a secondary mutation, a new library strain was tested. The *MATa ubp8* mutant (opposite mating type) was found to have a 2x decrease in the rate of direct repeat recombination compared to wildtype cells. This result suggests that the *MAT*α *ubp8* cells contain a secondary mutation that contributed to the hyper-intrachromosomal recombination phenotype, while the secondary mutation did not cause the EcoRI sensitivity within the cells.

Ubp8 is a protease that is involved in deubiquitination of histone H2B and is not active unless it is in complex with Sgf73, Sgf11, and Sus1 (DUBm complex). The DUBm mutants were tested for rate of intrachromosomal recombination (Table 6) and sensitivity to EcoRI (Figure 9). *sgf73* mutants displayed a substantial reduction in intrachromosomal recombination efficiency (21-fold), as well as a strong sensitivity to EcoRI expression. *sgf11* and *sus1* displayed WT phenotypes in both assays, with a very modest reduction in cell growth for *sgf11* after EcoRI expression.

All four DUBm mutants were then reconstructed in the lab using PCR-mediated gene disruption to avoid the potential effects caused by secondary mutations in the library strains. The new DUBm mutants were tested for bleomycin, MMS, and EcoRI survival.

ubp8 and *sgf73* were both sensitive to EcoRI expression, which suggests that the phenotypes seen in the library mutants were due to inactivation of the respective gene and not from a secondary mutation. The only mutant to display sensitivity to bleomycin was *sus1*, which exhibited a modest sensitivity compared to WT. All DUBm mutants displayed resistance to 2 mM MMS (Table 7).

The final goal of this project was to determine chromosome instability through loss of heterozygosity in the DUBm mutants. Four assays were initially designed with two heterozygous markers each. While two of the assay systems worked well for determining chromosome loss, it was determined that a three heterozygous marker system from Yoshida *et al.* (42) would be better to distinguish between chromosome loss and other types of events (Figure 18). *rad52* cells displayed a 40 fold increase in total LOH events and a much higher level of chromosome loss compared to WT (579×10^{-5} vs. 6.1×10^{-5}). *sgf73* and *sus1* cells displayed increased chromosome loss (66–73% of all events vs. 40% for WT) and approximately half the number of chromosome arm loss/allelic crossing over events seen in WT cells (24 and 32% compared to 56% in WT). *ubp8* and *sgf11* cells displayed chromosome loss frequencies similar to WT cells. All DUBm mutants displayed similar results as WT for local recombination (gene conversion) and small mutations (Table 8).

In summary, this project has led to the identification of several genes that are required for recombinational repair of DSBs and maintenance of chromosome stability. It is unclear why only a few of the 48 genes affect homologous recombination and whether the remaining genes affect NHEJ or not.

REFERENCES

1. Westmoreland, J. W.; Summers, J. A.; Holland, C. L.; Resnick, M. A.; Lewis, L. K. *DNA Repair* **2010**, *9*, 617–626.

2. Lewis, L. K.; Karthikeyan, G.; Cassiano, J.; Resnick, M. A. *Nucleic Acids Res.* **2005**, *33*, 4928–2939.

3. Hefferin, M.; Tomkinson, A. *DNA Repair*. **2005**, *4*, 639–648.

4. Ramotar, D.; Wang, H. *Curr. Genet.* **2003**, *43*, 213–224.

5. Sreedhara, A; Cowan, J. A. *J. Biol. Inorg. Chem.* **2001**, *6*, 337–347.

6. Xiao, W.; Chow, B. L.; Rathgeber, L. *Curr. Genet.* **1996**, *30*, 461–468.

7. Ma, W.; Westmoreland, J. W.; Gordenin, D. A.; Resnick, M. A. *PLoS Genet.* **2011**, *7*, e1002059. doi:10.1371/journal.pgen.1002059.

8. Williams, R. J. *Mol. Biotech.***2003**, *23*, 225–243.

9. Loenen, W. A. M.; Dryden, D. T. F.; Raleigh, E. A.; Wilson, G. G.; Murray, N. E. *Nucleic Acids Res.* **2013**.

10. Pingoud, A.; Jeltsch, A. *Nucleic Acids Res.* **2001**, *29* , 3705–3727.

11. McKinney, J. S.; Sethi, S.; Tripp, J. D.; Nguyen, T. N.; Sanderson, B. A.; Westmoreland, J. W.; Resnick, M. A.; Lewis, L. K. *BMC Genomics*. **2013**, *14*, 251.

12. Barnes, G.; Rine, J. *Proc. Natl. Acad. Sci.* **1985**, *82*, 1354–1358.

13. Khalil, A.; Morgan, R. N.; Adams, B. R.; Golding, S. E.; Dever, S. M.; Rosenberg, E.; Povirk, L. F.; Valerie, K. *Cell Cycle* **2011**, *10*, 481–491.

14. Ohnishi, T.; Mori, E.; Takahashi, A. *Mutat. Res.* **2009**, *669*, 8–12.

15. Lewis, L. K.; Kirchner, J. M.; Resnick, M. A. *Mol. Cell Biol.* **1998**, *18*, 1891–1902.

16. Symington, L. S. *Microbial. Mol. Bio. Rev.* **2002**, *66*, 630–670.

17. Wyman, C.; Kanaar, R. *Annu. Rev. Genet.* **2006**, *40*, 363–383.

18. Nakada, D.; Hirano, Y.; Sugimoto, K. *Mol. Cell Biol.* **2004**, *24*, 10016–10025.

19. Grenon, M.; Magill, C. P.; Lowndes, N. F.; Jackson, S. P. *FEMS Yeast Res.* **2006**, *6*, 836–847.

20. Bennett, C. B.; Lewis, L. K.; Karthikeyan, G.; Lobachev, K. S.; Jin, Y. H.; Sterling, J. F.; Snipe, J. R.; Resnick, M. A. *Genetics* **2001**, *29*, 426–434.

21. Game, J. C.; Birrell, G. W.; Brown, J. A.; Shibata, T.; Baccari, C.; Chu, A. M.; Williamson, M. S.; Brown, J. M. *Radiat. Res.* **2003**, *160*, 14–24.

22. Summers, J. A. Application of a Novel Endonuclease Sensitivity Assay to Identify New Genes that Affect DNA Repair and Chromosome Stability. M.S. Thesis, Texas State University, San Marcos, TX, 2008.

23. Sethi, S. Characterization of New Genes Required for DNA Double-Strand Repair in Saccharomyces cerevisiae. M.S. Thesis, Texas State University, San Marcos, TX, 2010.

24. DeMars, J. A. Use of a Novel Genomics Approach to Identify New DNA Repair Genes and Development of Improved Repair Assays. M.S. Thesis, Texas State University, San Marcos, TX, 2011.

25. Henry, K. W.; Wyce, A.; Lo, W. S.; Duggan, L. J.; Emre, N. C.; Kao, C. F.; Pillus, L.; Shilatifard, A.; Osley, M. A.; Berger, S. L. *Genes & Dev.* **2003**, *17*, 2648–2663.

26. Hochstrasser, M. *Annu. Rev. Genet.* **1996**, *30*, 405–439.

27. Ingvarsdottir, K.; Krogan, N. J.; Emre, N. C.; Wyce, A.; Thompson, N. J.; Emili, A.; Hughes, T. R.; Greenblatt, J. F.; Berger, S. L. *Mol. Cell. Biol.* **2005**, *25*, 1162–1172.

28. Lee, K. K.; Swanson, S. K.; Florens, L.; Washburn, M. P.; Workman, J. L. *Epigenetics Chromatin* **2009**, *2*, 2.

29. Samara, N. L.; Datta, A. B.; Berndsen, C. E.; Zhang, X.; Yao, T.; Cohen, R. E.; Wolberger, C. *Science* **2010**, *328*, 1025–1029.

30. Goldstein, A. L.; McCusker, J. H. *Yeast* **1999**, *15*, 1541–1553.

31. Soni, R.; Carmichael, J.P.; Murray, J.A. *Curr. Genet.* **1993**, *24*, 455–459.

32. Gietz, R. D.; Schiestl, R. H.; Willems, A. R.; Woods, R. A. *Yeast*. **1995**, *11*, 355–360.

33. Tripp, J. D.; Lilley, J. L.; Wood, W. N.; Lewis, L. K. *Yeast* **2013**, *30*, 191–200.

34. Lõoke, M.; Kristjuhan, K.; Kristjuhan, A. *Biotechniques* **2011**, *50*, 325–328.

35. Lee, C. K.; Araki, N.; Sowersby, D. S.; Lewis, L. K. *Yeast* **2012**, *29*, 73–80.

36. Lea, D. E.; Coulson, C. A. *J. Genetics* **1949**, *49*, 264–285.

37. Roberts, R. Development of New Assays to Identify *Saccharomyces cerevisiae* Genes Required for Efficient Repair of a Single Site-Specific DNA Double-Strand Break. M.S. Thesis, Texas State University, San Marcos, TX, 2008

38. Lee, K. K.; Florens, L.; Swanson, S. K.; Washburn, M. P.; Workman, J. L. *Mol. Cell. Biol.* **2005**, *25*, 1173–1182.

39. Kapitzky, L.; Beltrao, P.; Berens, T. J.; Gassner, N.; Zhou, C.; Wuster, A.; Wu, J.; Babu, M. M.; Elledge, S. J.; Toczyski, D.; Lokey, R. S.; Krogan, N. J. *Mol. Syst. Biol.* **2010**, *6*, 451.

40. Bahmed, K.; Seth, A.; Nitiss, K. C.; Nitiss, J. L. *Nucleic Acids Res.* **2011**, *39*, 970–978.

41. Kastenmayer, J. P.; Ni, L.; Chu, A.; Kitchen, L. E.; Au, W.; Yang, H.; Carter, C. D.; Wheeler, D.; Davis, R. W.; Boeke, J. D.; Snyder, M. A.; Basrai, M. A. *Genome Res.* **2006**, *16*, 365–373.

42. Yoshida, J.; Umezu, K.; Maki, H. *Genetics* **2003**, *164*, 31–46.

43. Song, W.; Petes, T. D. *Genetics* **2012**, *191*, 279–84.

44. Kumaran, R.; Yang, S.Y.; Leu, J.Y. *PLoS One* **2013**, *8*, e68094. doi:10.1371/journal.pone.0068094

45. Alabrudzinska, M.; Skoneczny, M.; Skoneczna, A. *PLoS One* **2011**, *6*, e21124. doi:10.1371/journal.pone.0021124